Philipps University Marburg

Department of Geography

Mapping of alpine treelines by using high-resolution aerial images and LiDAR data

Bachelor Thesis

Supervisors:

Prof. Dr. Maaike Baader

Dr. Hanna Meyer

Submitted by:

Jan Niclas Schwalb

Submission date:

December 10th 2018

Abstract:

Aim:

Treeline patterns could be an indicator for ecological processes and dynamics. To observe large areas a cost effective mapping method is needed. The aim of this approach is to use high-resolution aerial images combined with LiDAR data to identify individual trees, classify the species and derive the tree height for every individual tree. This could be used to reduce the time and cost expenditure to map and observe alpine treelines. The results will be statically evaluated with the previously collected ground truth data.

Methods:

A tree segmentation was performed to locate individual trees. The results of a basic watershed algorithm and a watershed region growing algorithm were compared. With a spectral classification, the two occurring species were separated by the specific wavelength of their spectral reflection. For every tree the height was added through LiDAR derived data. All derived data was statistically evaluated by the previously digitized field data to check the accuracy of each segmentation method.

Results:

The spectral classification showed different results due to the different number of detected entities in each structural segmentation. The basic watershed method segmented 67.5% of the occurring tree individuals and predicted 92.6% of the species correctly. The watershed region growing method segmented 90% of the occurring tree individuals and predicted 91.7% of the species correctly. The remote sensing derived tree heights are strongly correlating with the ground truth data.

Main conclusion:

In this case the vegetation is very heterogeneously distributed consisting of small trees as well as big trees. This leads to crown splitting of bigger trees and to the ignoring of small trees. The results are although pretty accurate especially with regards to the watershed region growing segmentation algorithm. The species identification works also sufficiently and the highly correlating tree heights leads to the assumption that remote sensing derived data is a reliable tool to complement field investigation and prediction. A rising data availability and accuracy will enable a more realistic observation of alpine treelines.

Table of contents

1. Introduction

The framework of this work contains many disciplines which are linked to various departments of research. "Forest ecosystems cover about 30% of our planet, account for 75% of the gross primary productivity of the Earth's biosphere, and contain 80% of the Earth's plant biomass" [Dalponde et. al. 2015]. Forestry is a large economic factor and the execution of forest inventory evaluation is a time and cost intensive undertaking. On an ecological point of view it is also an ongoing research to define the driving factors of limited tree growth in different degrees of latitude. The fact that the global temperatures are rising since the Industrialization, show rapid and well documented changes in highly sensible and temperature dependent ecosystems including alpine treelines [Solomon et al. 2007]. A monitoring of these processes is cost and time expensive to perform on a bigger scale. Instead to determine every relevant parameter per field investigation, modern remote sensing equipment and more powerful computing conditions like machine learning algorithms enables the possibility to determine these parameters without the physical presence of evaluating professionals. Remote sensing provides in some parameters even a more precise and cost effective alternative to field investigations [Grafström & Ringvall 2013]. But there will always be a need to do field investigation due to the fact that every predicted feature has to be empirically validated.

1.1 Aerial image based classification

The most common way to classify tree species is the use of multispectral sensor based aerial images. These multispectral sensors not only contain the standard RGB (red, green, blue) bands we use for true color images, it also contains near infrared (NIR) bands. The more NIR bands a sensor contains, the more spectral properties of the observed area and its containing objects can be specified more precisely. Every NIR band covers a certain range of infrared wavelengths which could be used to find a specific wavelength which matches the best way to classify a certain objects wavelength and fencing it of other objects . Every kind of vegetation has a specific spectral reflection due the absorbing and reflecting properties of the Chlorophyll composition in plant leaves. The spectral wavelength of NIR channels is the best way to classify vegetation and fencing it off non vegetation objects (Dalponte et al., 2009]. There a numerous indices which are using slightly different variations of NIR band combination and also some based on RGB band variations. In this particular case we want to

identify and classify the tree species *Larix decidua* and *Pinus uncinata*. A important limiting factor of infrared image based classification is the high financial expenditure. To cover larger objects of interest, it may be sufficient to use free or less expensive available satellite imagery (MODIS, Landsat8 and many more existing and in development). But to classify smaller objects like small trees and shrubs, researchers rely on high resolution aerial imagery. But working with high resolution multispectral imagery sometimes requires a high project budget which may prevent motivated researcher in low budget projects to work on their interest. Neither existing data (if plane based aerial or satellite imagery) nor actual plane based orders (Aerial image company contract e.g.) are an option for small departments. But there are some serious attempts to classify vegetation only with relatively cheap RGB sensors. The "Nature 4.0" project aims to monitor complex natural entities with low budget equipment [Natur 4.0 2018]. One part of the research is focused on UAV based (unmanned aerial vehicle) high resolution RGB image mapping, also dealing with RGB based classification of multiple tree species [Reudenbach 2018a]. In this work the spectral classification will also be performed by using RGB imagery without NIR bands.

1.2 LiDAR point cloud based object segmentation

The method of Light Detection and Ranging (LiDAR) or also called Airborn Laser Scanning (ALS) is widely used to detect and measure objects on three dimensional surfaces (Kaartinen et. al.). Mostly these data is gathered by planes or sometimes helicopters which are emitting lasers to the ground and calculate the height by the time the laser takes to reflect back to the sensor. Some of these lasers manage to get through vegetation and reflect from the ground which enables to measure vegetation heights and other associated parameters. In recent years the use of LiDAR data is increasingly used to predict forest inventory and even parameters like the stem diameter at breast height (DBH) for individual trees (Mohan et. al 2017). In this work the trees will be segmented as individuals by two different segmentation algorithms. A basic watershed algorithm based on the introduction by Popescu and Wynne 2004 and a watershed region growing algorithm based on the introduction by Hyyppä et al. 2001 will be applied. The results will be compared to decide which algorithm performs better to segment heterogeneously distributed trees of different sizes.

1.3 Alpine treelines

The well known phenomenon of decreasing tree growth in high altitudes is a point of interest for researchers around the world for a long time. Many theories exist to describe this fact from many points of view and different scientific areas. The altitude where trees could grow differs depending on which degree of latitude the study area is located. Also the influence of global warming is a factor that leads to changes in these highly sensitive environments [Harsch et. al. 2009]. It is important to monitor these ecosystems to predict changes on a global scale. But the fact that alpine treelines are mostly located on remote places makes it more costly to research than other related topics. The future might ease these issue by the use of remote sensing. The accessible data gets more detailed and enables to detect even very small crippled tree individuals or predict parameters of a tree where it is too dangerous to go for researchers. In this work, the existing treeline at the study area was identified and classified by remote sensing data. The remote sensing derived tree species and tree heights were compared with the field data to check the data accuracy. Significant results could help to monitor processes like new establishing of seedlings or the vanishing of known trees by remote sensing.

2. Methods:

2.1 Data preprocessing:

Field data:

In this work, exclusively the geographical information system (GIS) "ArcGIS" and the open source application "R-Studio" were used. During the field investigation all necessary data was raised within a 220 x 30 meter plot, divided up eight 30 x 30 meter subplots along a steep partially forested hill slope. The plot is located near the city of Grenoble in the French Alps (Fig. 1). Within this plot every tree including their position, species and tree height were detected and recorded as well as other parameters which were not used in this work. The tree positions were detected by global positioning system (GPS) coordinates and as well with X,Y,Z coordinates relative to the created plot. This ensures that even if the GPS Signal has a lack of accuracy, the trees could be located manually in relation to the plot and its objects. In the whole plot 40 individual trees were recorded. The tree heights vary between 1.2 and 11.4 meters and a have mean height of 5.4 meters. Eleven individuals of *Larix decidua* and 29 *Pinus uncinata* were recorded. The elevation height above the sea level differs within the plot between about 2100 to 2400 meters.

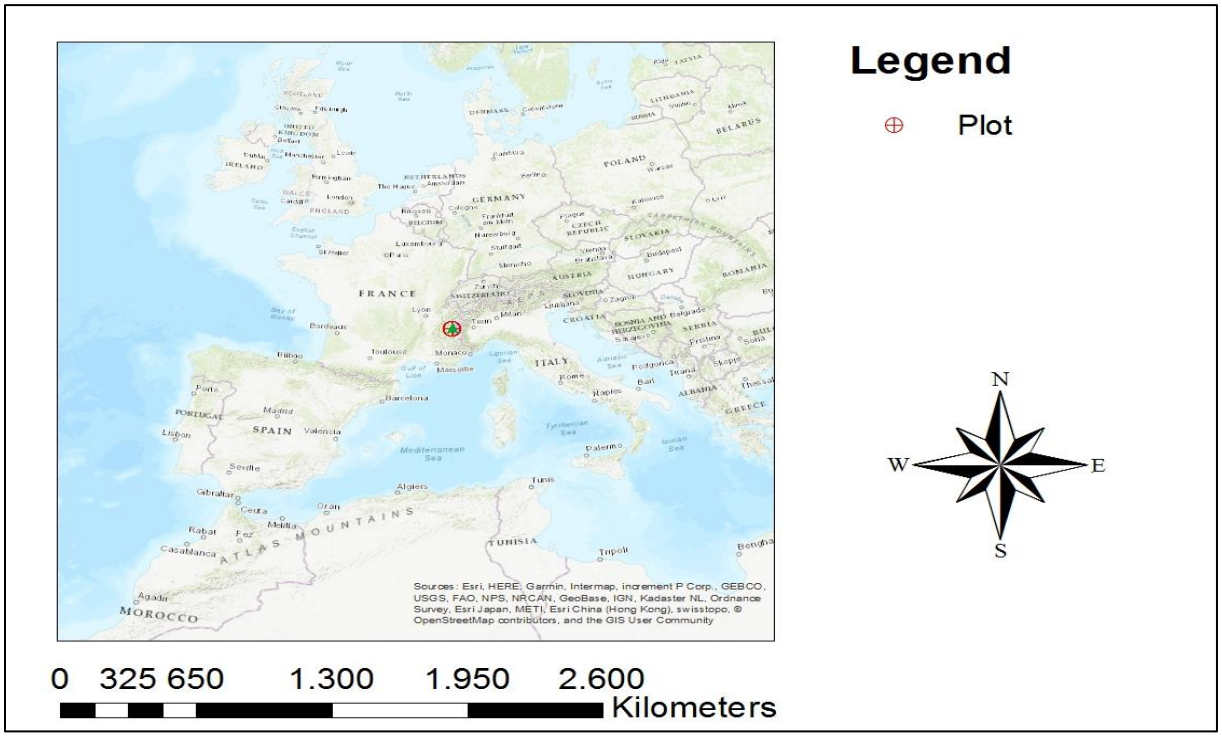

Fig. 1: Plot position large scale

Field data digitizing:

For further calculations the field data was digitized in order to validate the following results derived by remote sensing data. All data was converted into an Excel chart containing all raised information. The GPS coordinates of the plot corners were used to create a grid feature layer of the plot to help assigning the trees to their exact position. Because the accuracy of the used GPS trackers was not precise enough to ensure the exact tree position, some trees were located by the X,Y,Z coordinates based grid relatively to the previously collected objects. The tree coordinates were then used to create a point feature layer containing all collected information for every single tree (Fig. 2).

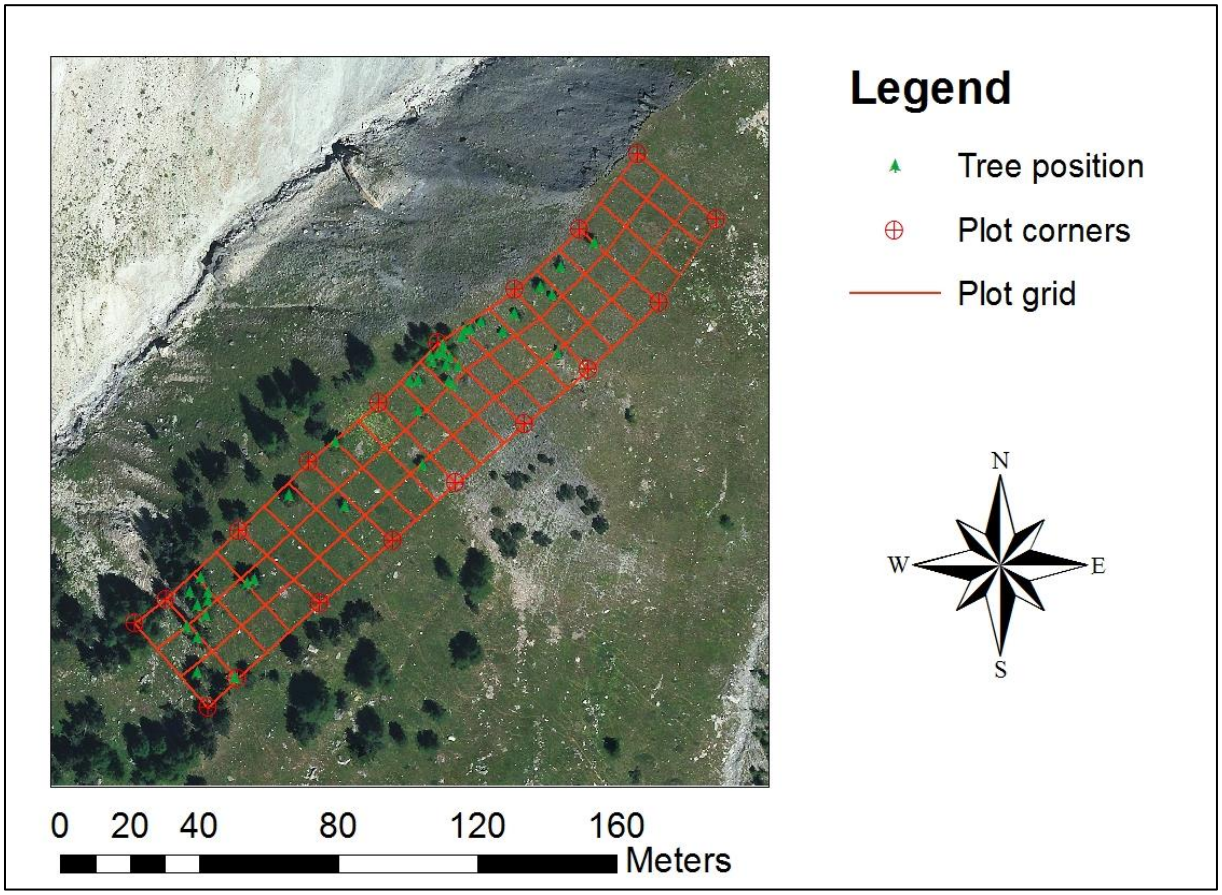

Fig. 2: Digitized plot and tree positions

Coordinate system projection of remote sensing data

All available data was projected into the same coordinate system. In this case the French regional coordinate system "*RGF_1993_Lambert" (EPSG: 2154*) was used to get a consistent spatial accuracy for all used data sources. As a result the aerial RGB images, the LiDAR data and the digitized field data features were projected into the same coordinate system for further processing.

Clip and merge remote sensing data to preferred extent

The used aerial RGB images have a 0.15 x 0.15 meter resolution. The LiDAR point cloud density allows to create a 0.5 x 0.5 (~4 points per m^2) meter raster resolution. The RGB image contains three spectral bands (Red, Green, Blue) and the LiDAR point cloud has predefined ground and surface layers. In order to minimize the calculation expenditure in further steps, the extent of the RGB images was reduced to an area slightly bigger than the field plot and the smaller tiles were merged into one great tile. For the LiDAR tiles (provided in .LAS format) we waited for further processing steps where the point cloud data was converted into raster data. But if one wants to take a look into the raw data (point cloud) without choosing all desired LAS tiles, there is a third party toolbox, called "LAStools" which provides useful tools to merge many tiles into one [Isenberg 2018]. In this case it was not performed because the area of interest and the LiDAR tiles were too small to caused any significant rise of processing time. But for analyzing larger areas it makes sense to clip the point cloud to save unnecessary processing expenditure. Another good way to access the LAS files "on the fly" (that means it saves memory because only the needed files occupy disk space) is to handle the data in an index catalog [Roussel 2018b]. With this method large LiDAR data can be handled without getting memory and processing issues.

2.2 Processing spectral RGB image classification:

The first step to get unique spectral values for each tree species is to segment the RGB Image. This way, the spectral properties are simplified into more generalized values with a thinner spectrum of pixel value diversity. While a tree contains a lot of different values within an RGB image (three band with values ranging from 0 to 255), an segmented RGB image contains lower value scattering and detail depth. With this way it is more convenient to find a value composition which represents an individual spectral reflection for a species. To do so, a segment mean shift algorithm was used to flatten the detail depth (Fig. 3). To get the right spectral and spatial accuracy, some values were tried out to find a matching combination suitable for the composition of the plot . In this case we needed high spectral and medium spatial accuracy. But the higher the details are, the more small patches were calculated. That is a problem because in this case we more likely to need bigger patches which should help to classify trees. These values proved to bring the best results: Spectral detail: 18/20 ; Spatial detail: 14/20 and a minimum segment size of 30 pixels (1 pixel = 15 x 15 cm). The minimum segment size was chosen because the smallest tree within the plot has a crown area of about that size.

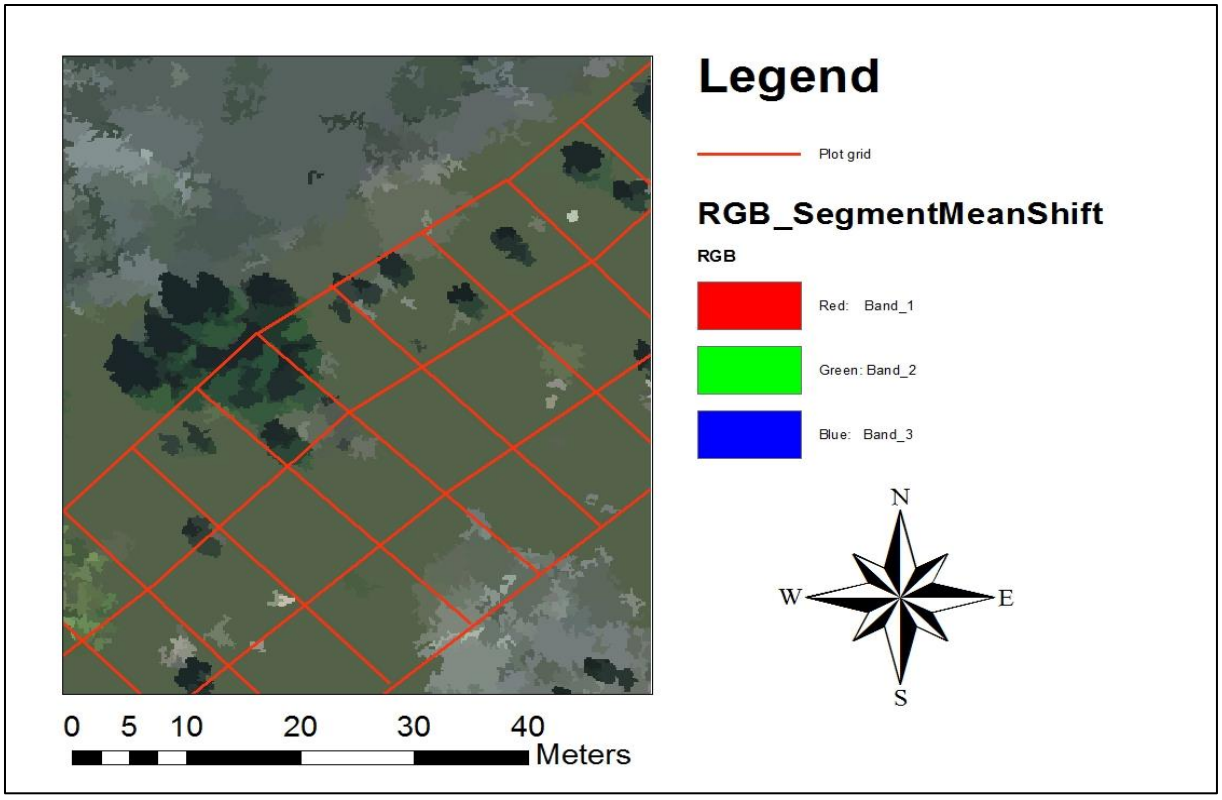

Fig. 3: Segment mean shift algorithm RGB smoothing

The following procedure is to create training areas which will be used by an classification algorithm called "maximum likelihood classification". These training areas should cover the major occurring segment values. Of course there a numerous approaches to perform a spectral classification. Perhaps the best solution is to use a machine leaning algorithm like "Random Forest" or one of many other similar solutions. In this case the maximum likelihood classification is a sufficient solution because there are only two species which we want to recognize and differentiate. Supported by the field data and visual control on the original RGB image, training areas were expelled for the spectral classes: Pinus, Larix, meadow, Basalt rock, Chalk rock, and large herbs. A major problem in nearly all aerial image based classifications are shadows. Shadows distort the spectral reflection of objects. This causes that shadowed areas of one individual tree were interpreted as a different spectral class. A good way to avoid this issue is to use aerial images from different times of a day. This way shadow covered areas were dismissed on one image and instead the shadow free parts of the other image were used.

Another great way which requires some skills in programming is a false color recalculation, where the RGB image is converted into a "YCbCr" false color image and shadowed areas gets lighted up [Deb & Ashraful 2014]. But in this case no additional aerial images or the required skills to perform a shadow pixel relighting were available. A method was chosen where shadowed areas simply were expelled as a land use class training area and then erased. Though this leads to a loss of data it helps to get rid of distorting spectral information. In sunny areas the spectral reflection of Pinus and Larix is different enough to distinguish each species. The problem in this case is that shadowed Larix areas have a similar reflection as sunny Pinus areas. We want to avoid that, so we created additional training areas to get rid of shadows. Additional four classes were created for "Larix_sunny" , "Larix_shadow" , "Pinus_sunny" and "Pinus_shadow". The created training areas were used by the maximum likelihood classification algorithm to create a classified raster.

We have a classified raster with the desired classes: "*Larix_sunny*" , "*Larix_shadow*" , "*Pinus_sunny*" and "*Pinus_shadow*". But the raster also contains the other classes we do not need for further processing and tree classification. To get rid of those undesired classes (Meadow, Basalt_stone etc.) their pixel value was set to no value. We do not need the classes "*Larix_shadow*" and "*Pinus_shadow*" either because we only want to look at the sunny areas which are most suitable for classification . Therefore, the shadow areas were set to "no value" as well. As a result we only have the areas of which we know they are representative for the spectral reflection of the individual species. All the surrounding areas have no values (Fig. 4). To get rid of misclassified areas (e.g. meadow classified as Larix), we used the (later calculated) canopy height model (CHM) to get rid of classified pixels which are below 0.7 meters (a bit lower than the lowest tree height). This is the spectral classified product we later need for assigning the species (spectral classification pixels) to a segmented spatial structure (polygons derived through LiDAR data processing) which we then could call an individual tree.

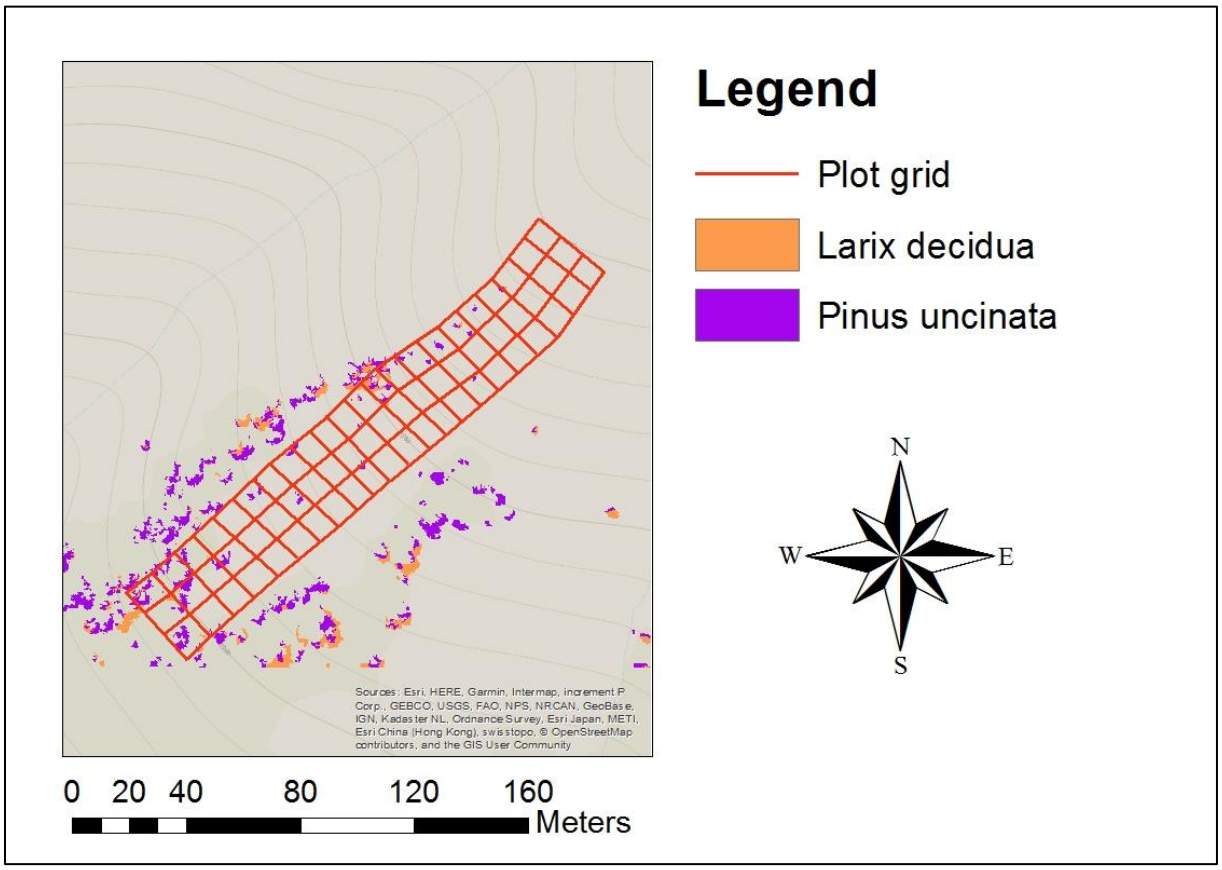

Fig. 4: Classified raster with only Pinus and Larix pixels

2.3 Preprocessing structural LiDAR point cloud segmentation

Preprocessing LAS files

In order to process the spatial information provided by the LAS files, an LAS dataset was created. For this case the data was separated in two files containing the ground and non ground (surface) returns. The derived datasets were corrected in order to get rid of potentially distorting values. Those undesired values lay beneath zero meters and beyond 25 meters (ground and maximum tree height). These values could be caused by falsely interpreted LiDAR pulse returns, flying birds, blown up tree leaves or other interfering objects. A ground point return detection was used to perform a morphological filter for removing non ground returns from the surface return layer in order to erase eventually wrong predefined points [Zhang et.al 2003].

Computing digital elevation/surface model

With these two corrected LAS datasets a digital elevation model (DEM) from the ground return LAS dataset and a digital surface model (DSM) from the non ground return LAS dataset was derived. A digital elevation model contains only ground returns and filters out any kind of vegetation (Fig. 5). The digital surface model also contains the returns which includes ground and vegetation (Fig. 6). To do so, the LAS dataset was converted into a surface (DSM) and ground (DEM) raster. It is important to set the "Cell assignment type" for the DEM to "*average*" and for the DSM to "*maximum*". The accuracy of the LAS tiles allowed to set a 0.5 x 0.5 meter pixel size resolution for the processed rasters.

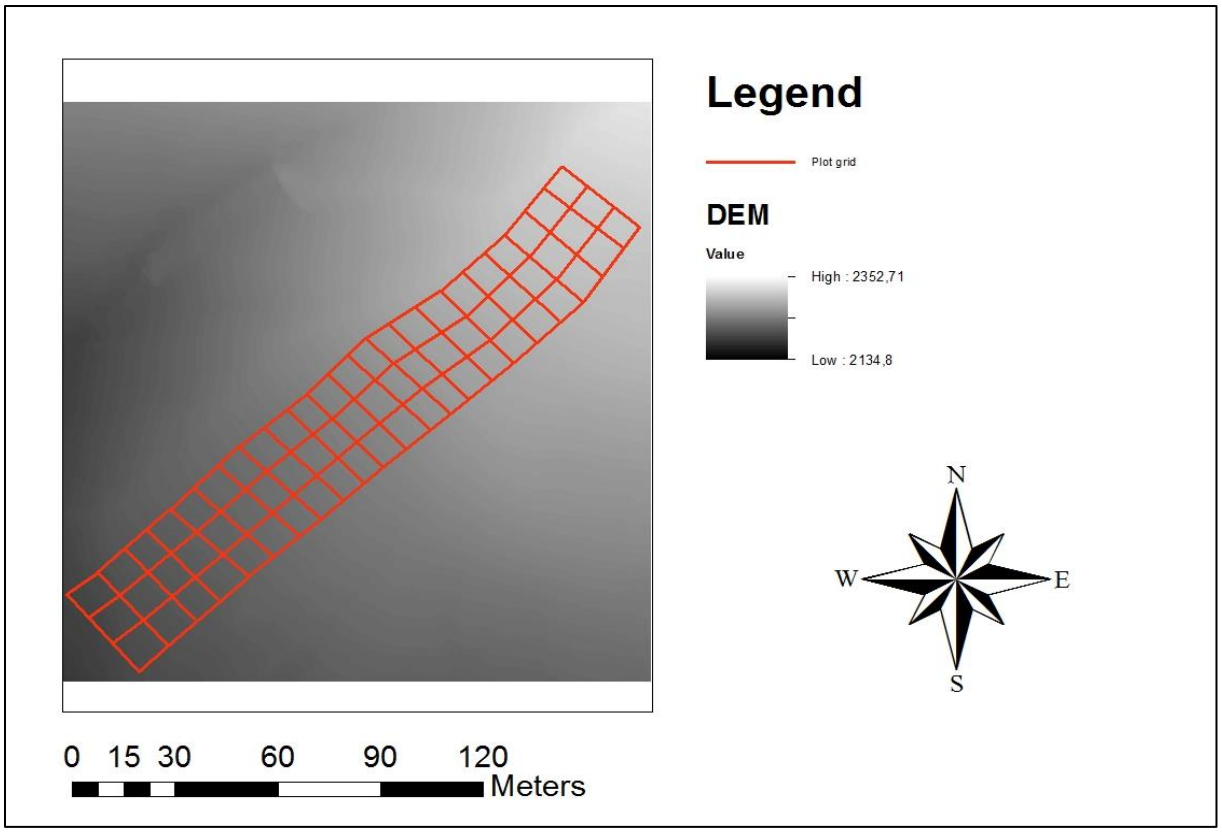

Fig. 5: Digital elevation model (DEM) of the plot area

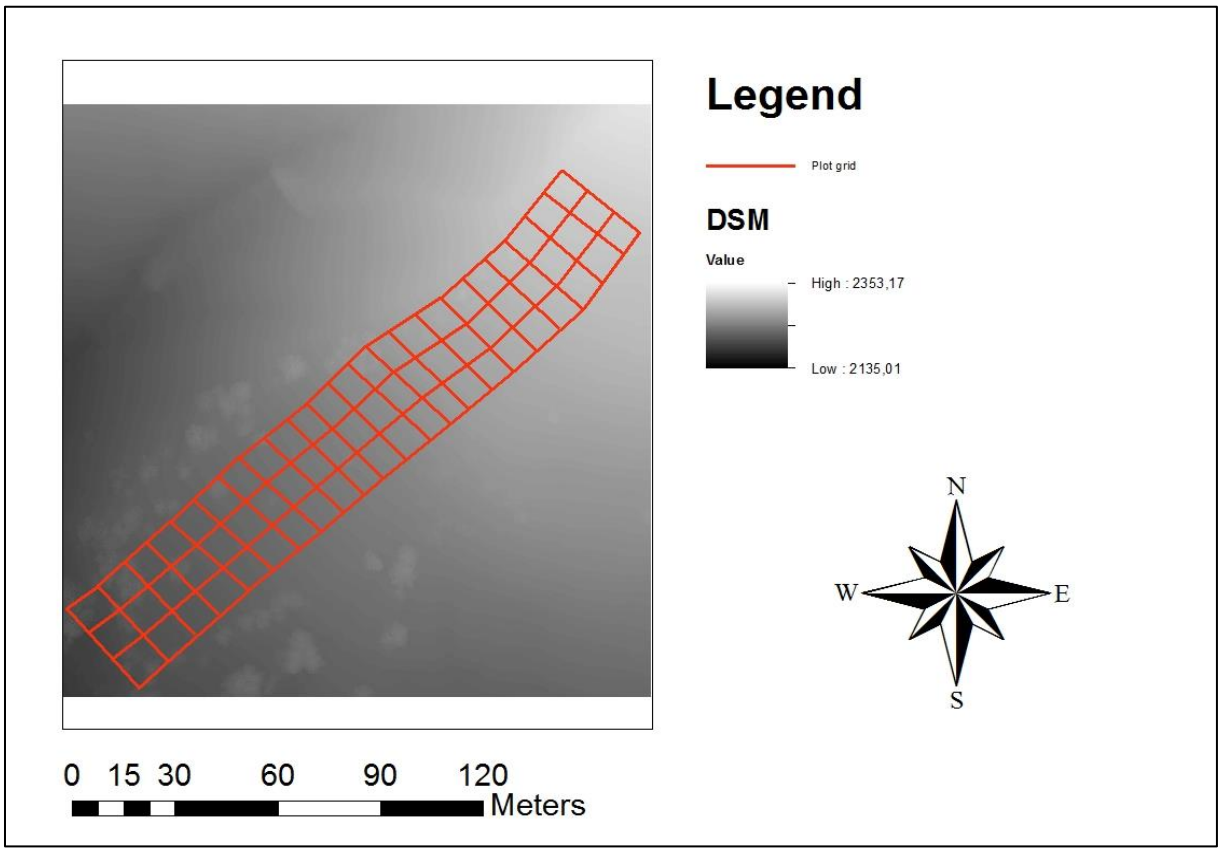

Fig. 6: Digital surface model (DSM) of the plot area

Computing canopy height model

To extract tree heights a canopy height model (CHM) was derived . This was done by subtracting the DEM from the DSM. As a result, we got a raster where every pixel value represents the height (0-28 meters) over the ground (Fig 7). A better way to handle this kind of processing is to use the application "R-Studio" instead of other geographic information systems like "ArcGIS" or "QGIS". There are many solutions provided in numerous R packages. In this case the "lidR" package was used to grid the canopy [Roussel 2018a]. The implemented algorithm is based on the pit free CHM algorithm [Khosravipour et. al. 2013]. To smooth the CHM raster, a filter was used to refine the pixel resolution (10 x 10 cm) in order to improve the border accuracy between tree height pixels (CHM) and ground pixels. To eliminate negative values, a conditional function was used to drop values beneath zero in the CHM raster. The edited CHM has no distorting values which could possibly interfere with the following tasks.

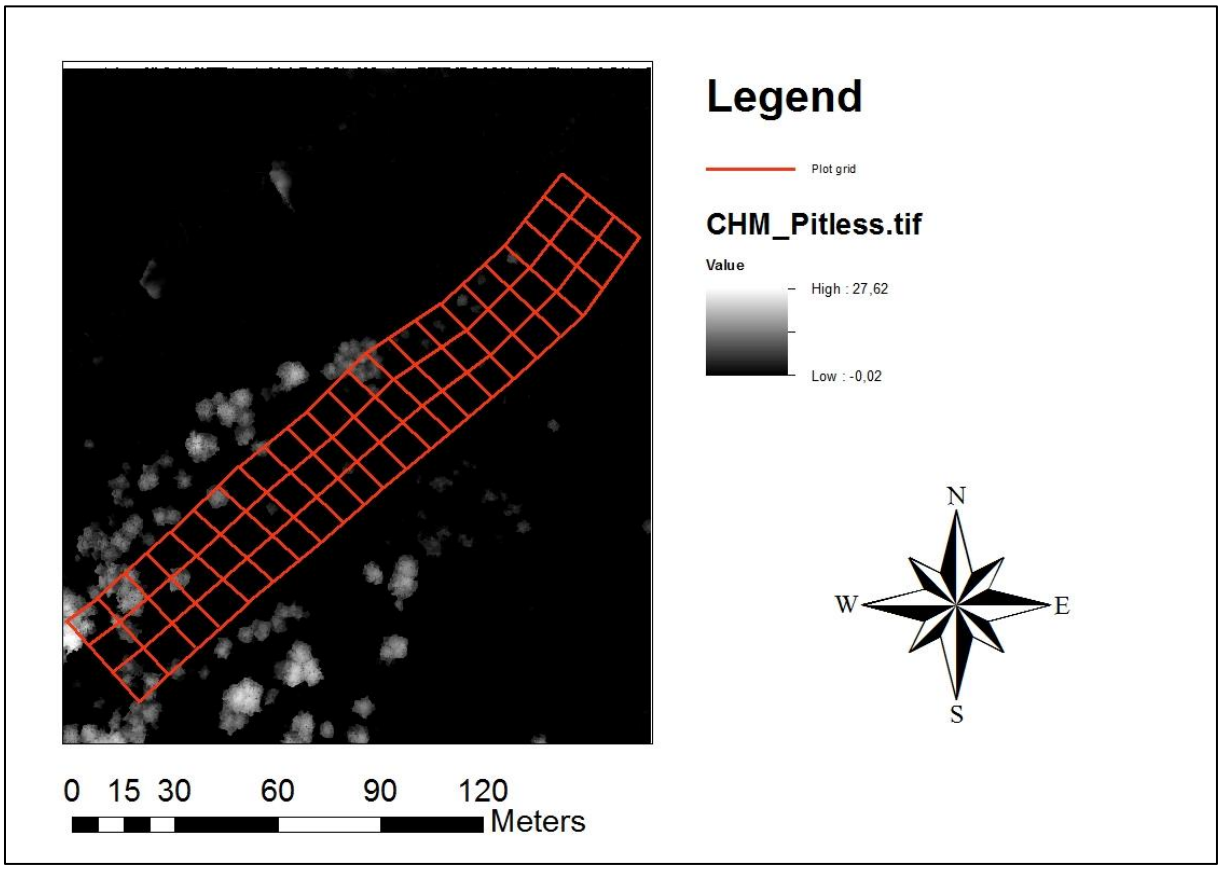

Fig. 7: Canopy height model (CHM) of the plot area

Apply structural crown segmentation

There are numerous segmentation algorithms to identify tree crowns. Many of them work with a similar procedure called "watershed segmentation". This segmentation type uses a simulated water flow to define sinks where the water accumulates. The common way is to invert the CHM by multiplying it with minus one (-1) using the raster calculator. After this step all positive values (pixels with numeric tree height value) are converted to negative values. With a fill function, simulated water is poured into the inverted CHM. The calculation of flow accumulation and flow direction were used to define areas where the simulated water accumulates and from which position the accumulation takes place. With a watershed function, the calculated rasters were used to convert areas of accumulation into polygons which represent tree crowns [Trent University 2014]. This could be a quietly click intensive workflow when using GIS software like QGIS or ArcGIS. A more convenient way is to use an algorithm where you can change the values more quickly to find the best suiting parameters for the area of interest. On Github are many free available packages which contain functions for numerous segmentation algorithms coded for R. For this case, two (out of numerous slightly distinguished from each other) segmentation algorithms were compared to choose the best fitting solution to detect very small trees as well as bigger trees.

2.4 Watershed based segmentation algorithm

The first method is a basic watershed algorithm as described before. It is based on a canopy height model and a tree position layer where local maxima were derived [Koch et. al. 2006]. The method is implemented in the "lidR" package for R-studio and the function is called "lastrees" (Roussel 2018c). The threshold for detecting trees was set to 0.7 meters corresponding to the smallest tree detected in the plot. The input data is the previously created canopy height model. Additionally it is combined with a tree position raster where local maxima were calculated. In this case it does not work that well enough because of the heterogeneous tree heights. Either big trees get split into more polygons or small trees were not detected (Fig. 8). But for homogeneous forests with similar tree sizes this algorithm is expected to work better.

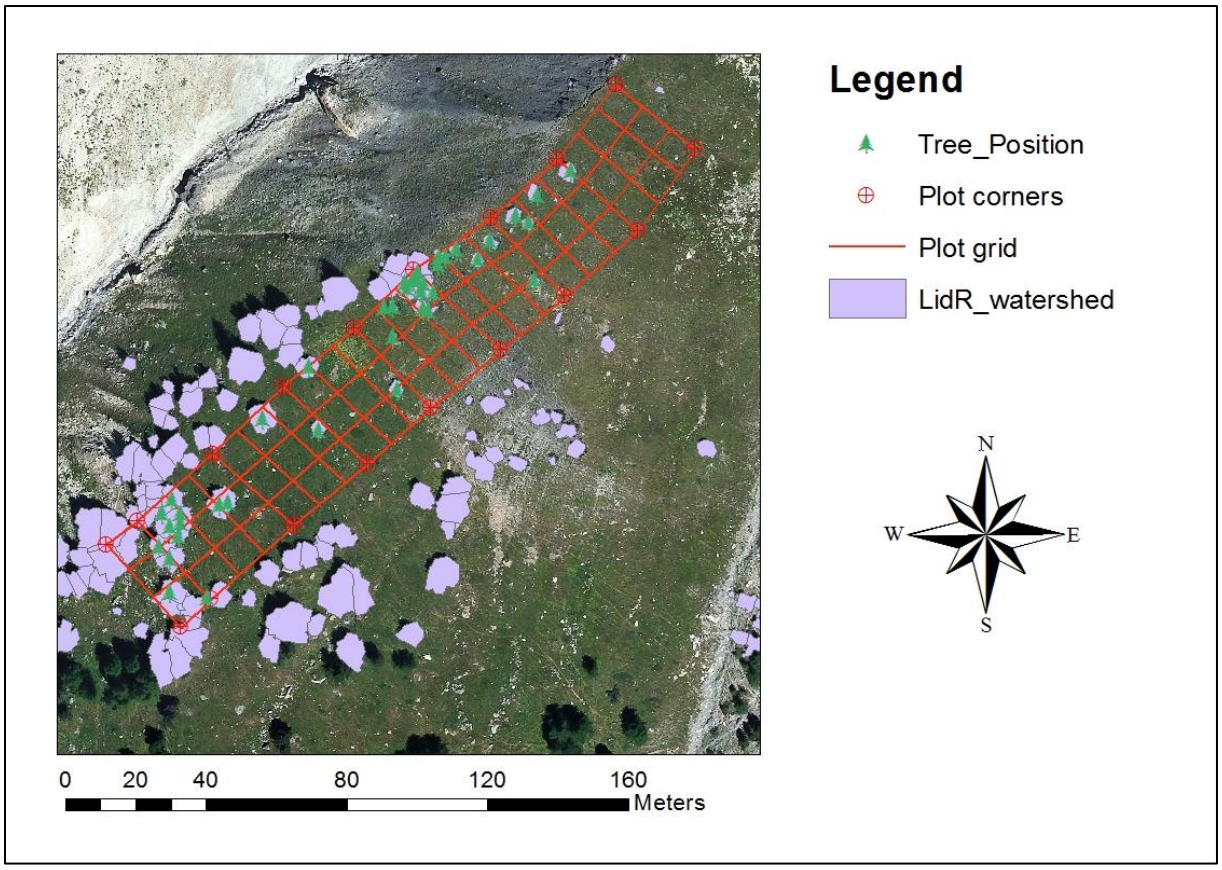

Fig. 8: Watershed based segmentation algorithm derived polygons

2.5 Watershed region growing segmentation algorithm

This algorithm is based on an individual tree crown (ITC) delineation method introduced by Hyyppä et al. 2001. This is a slightly varied method which was first introduced by Ene et. al. 2012 and improved by Dalponte et. al. 2015. "The ITCs are firstly defined on the raster CHM using a watershed method and then they are reshaped using the normalized point cloud." [Dalponte et. al. 2015 p: 369] This is called an "watershed region growing algorithm" and a special feature is the possibility to calculate overlapping tree crowns. The algorithm is implemented in the "uavRst" package, provided in the function "chmseg_ITC" (Reudenbach 2018b). The implemented algorithm is a variation of the Dalponte et. al. 2015 and also contains a editable moving window for local maxima detection. The original algorithm has a fixed 3x3 moving window. In this case, after trying different variations, a moving window of 15 pixels, a maximum crown area of 150 square meters and a minimum tree height of 0.7 meters was used (Fig. 9). In this case problems occurred in form of crown splitting of big trees.

The required steps of this method is best described by Dalponte et. al. 2015 as follows:

1. a low-pass filter (LPF) is applied to the raster image of the CHM;
2. a watershed segmentation is applied to the filtered image, obtaining the image L of the segmented regions;
3. from each region in L the first return ALS points are extracted, and the Otsu thresholding method [Otsu, 1979] is applied to their normalized heights;
4. the first return ALS points higher than the Otsu threshold are extracted and a 2D convex hull is applied to these points;
5. the resulting polygons are the final ITCs.

[Dalponte et. al. 2015 p: 369]

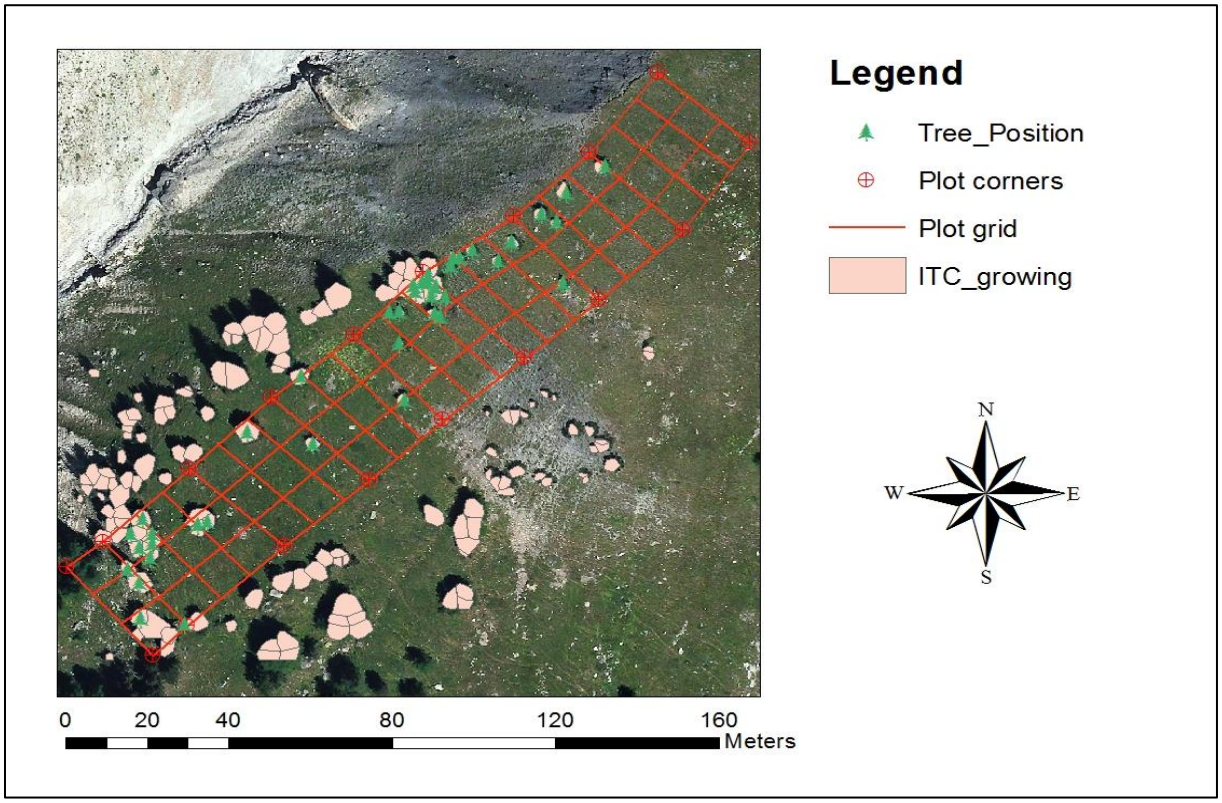

Fig. 9: Watershed region growing segmentation algorithm derived polygons

2.6 Preprocessing segmentation and value assignment

Clip segmented polygons to plot extent

Before discussing the results of this segmentation, the classified polygons were clipped to the extent of the plot (Fig. 10). The grid layer was used as a mask to cut out only those polygons which lay within or touches the grid layer.

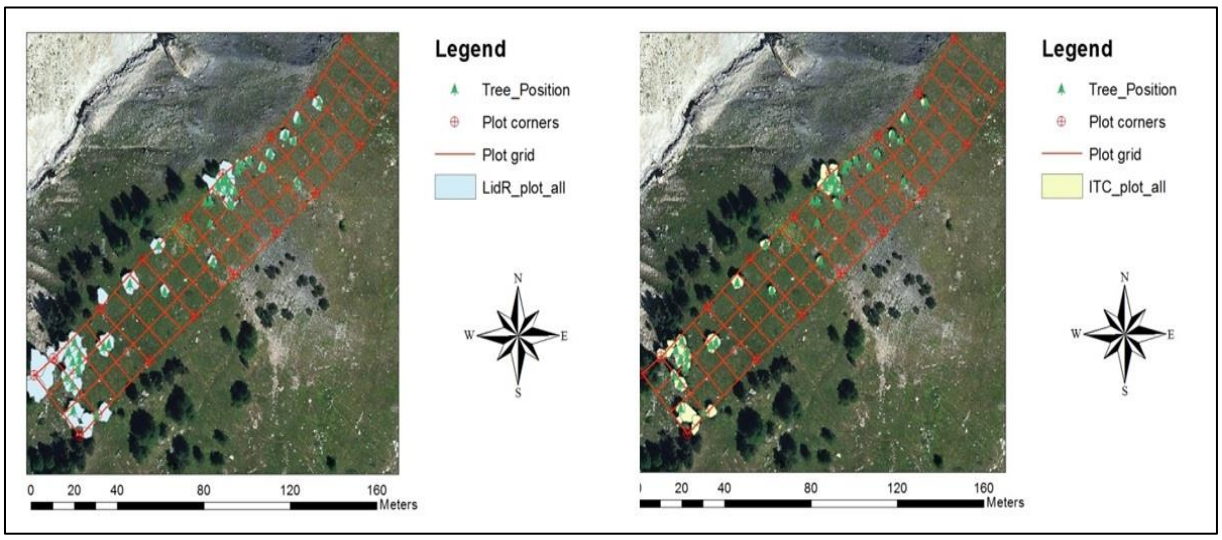

Fig. 10: Clip unwanted polygons to plot extent

Watershed-polygon preprocessing

It has to be examined if there were trees inside the plot which were not covered by field data. There are some yellow polygons which do not have a field data tree-ID assigned to them (Graph 12, yellow circle). There are 38 trees identified in the plot, from which 11 trees were not assigned to a single field data tree. These 11 polygons only contain the remote sensing derived species. This issue occurs because the location of the polygons in the edge area where the plot ends (Fig. 11). This happens because tree crowns overlapped into the area of the grid, but their stem laid outside and was therefore not included in the field investigation data.

There are no other misclassified trees within the plot. In this case we can delete these polygons and only have 27 polygons left, which represent all remaining 40 trees we identified during field investigation. This equals a single tree identification rate of 67.5 percent. Noticing that the corner areas of the lower plot were not investigated during the field trip, we erased these polygons in this area for evaluation (Fig. 12, yellow circle). There are two polygons which each contain four field data tree positions, two which contain each three tree positions and three which contain each two tree positions. These were the missing 13 trees. As a result we can see that many trees were combined into one because of the polygon sizes. We can also see that all trees were assigned to at least one polygon.

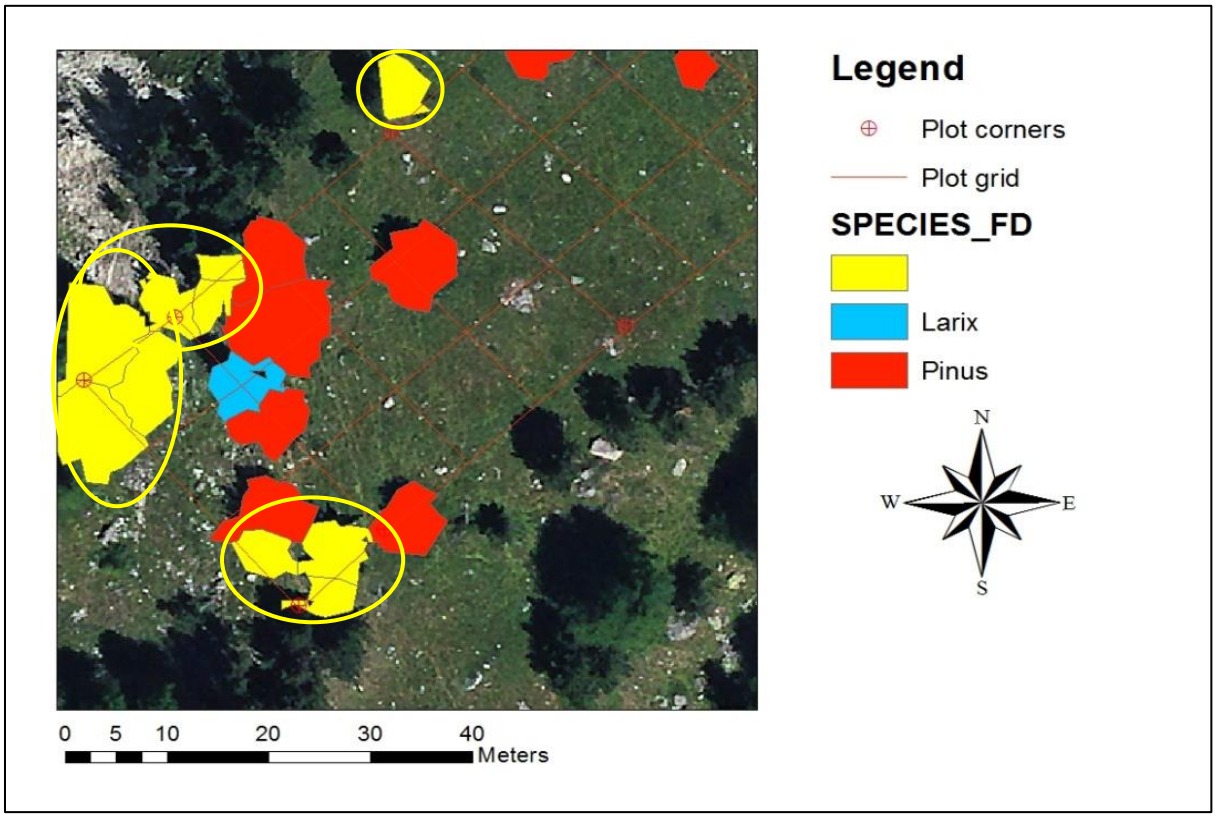

Fig. 11: Unclassified polygons within the plot area

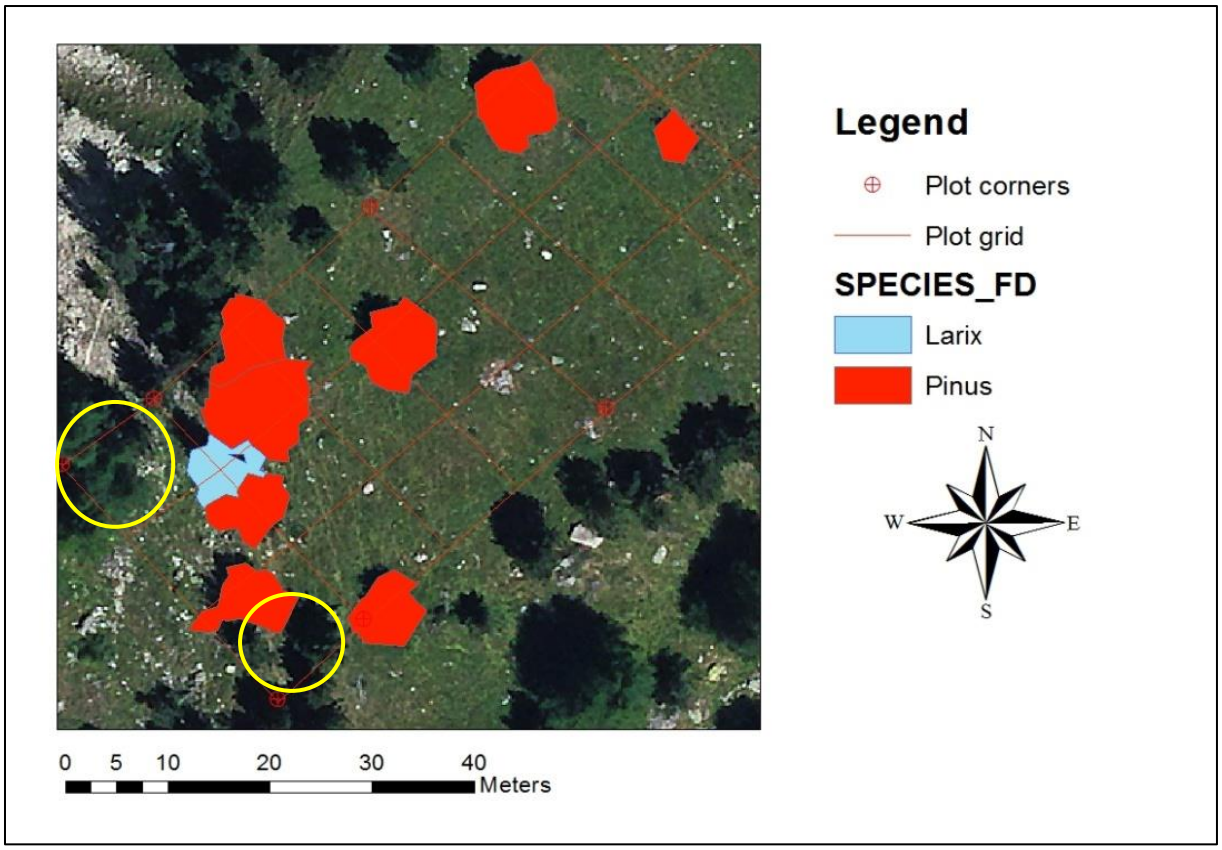

Fig. 12: Cleaned segments

Watershed region growing-polygon preprocessing

It has to be examined if there were trees inside the plot which were not covered by field data. The watershed region growing algorithm recognized 47 individual trees within the plot. That means seven trees more than identified during the field investigation. Eleven of them were not assigned to a field investigation identified tree (Fig. 13, yellow circle). In this case eight of them were created because of overlapping tree crowns into the plot and three of them resulted out of tree crown splitting of bigger tree individuals (Fig. 13, red circle). For further evaluation we have to erase these polygons. But we have to keep in mind that with this method three polygons were misclassified within the plot caused by tree crown splitting. 36 tree crown polygons out of 40 trees that were identified during field investigation were identified correctly (Fig. 14). This equals a single tree identification rate of 90%. But there are four tree positions lost. One of them lays out of any polygon and was not assigned to one. Three times, two tree positions were included into one polygon.

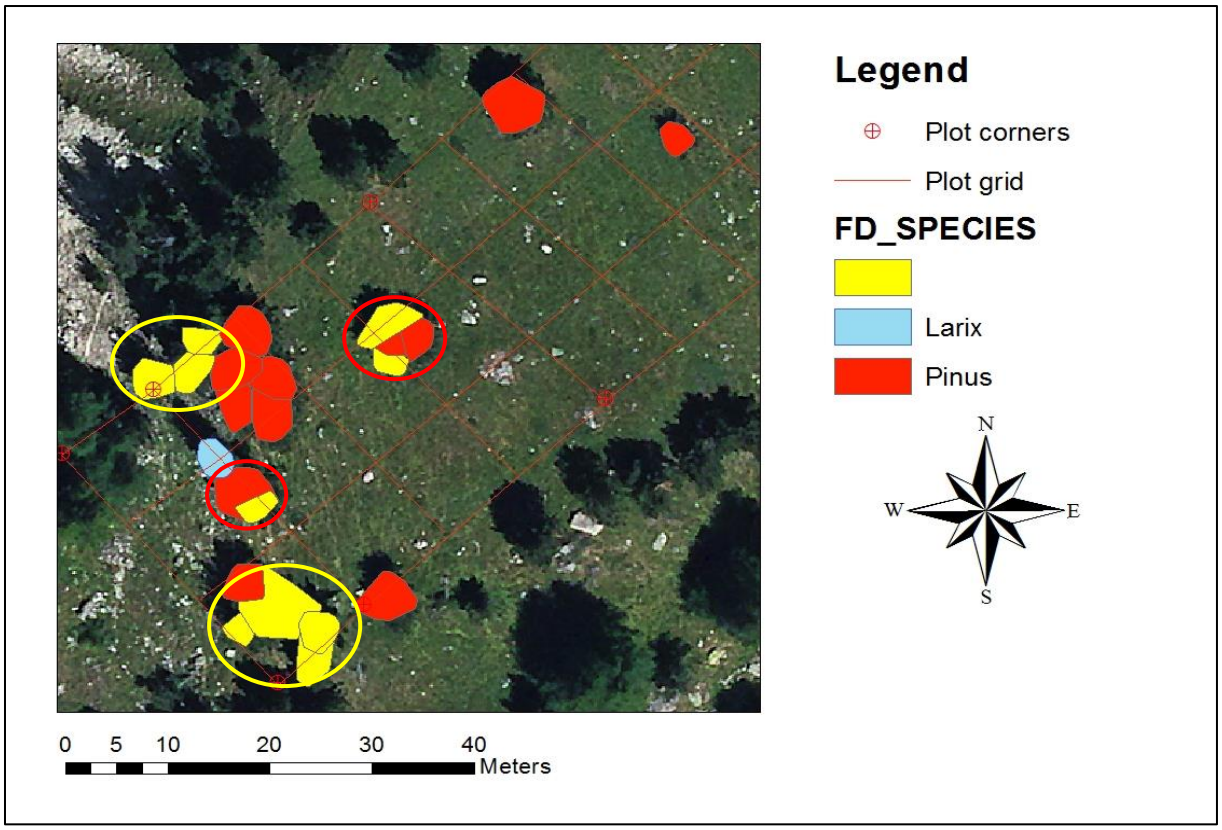

Fig. 13: Unclassified polygons within the plot area

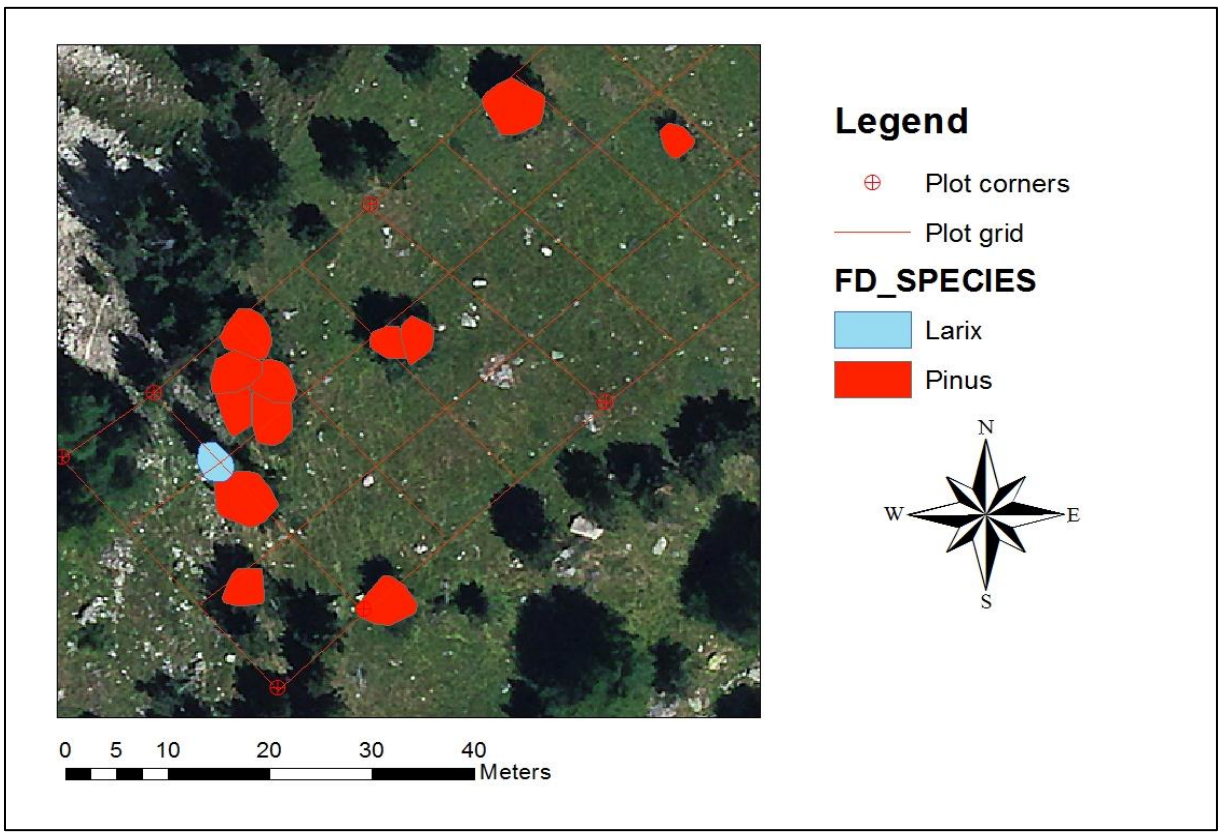

Fig. 14: Cleaned segments

Assigning spectral classification raster to structural segmentation polygons

In order to combine the previous derived spectral classification data with the structural tree crown segmentation, the raster values of the spectral classification raster were counted within each polygon of the tree crown segmentation. The "zonal statistics as table" tool (ArcGIS) provides the standard deviation, mean, majority and the minority statistics of the two classes "Larix" and "Pinus" within each polygon. If the classification pixels are more clearly distributed, the majority statistics is the best way to assign the spectral classified species to the polygon. But in this case, single trees contained both classes with a proportional higher amount of Pinus pixels. To deal with this issue the mean values were used to find a threshold value which differentiates the two classes most accurately. The pixel value of Larix is "2" and for Pinus "18". Mean values under 11 were classified in most cases as Larix and beyond 11 as Pinus. For the watershed algorithm a threshold value of 11.15 was applied. For the watershed region growing algorithm a threshold value of 16.5 was applied. The significant difference of these values occur due to the different polygon sizes of the structural segmentation. The polygon's size of the watershed algorithm is in most cases significantly bigger as the polygons derived by the watershed region growing algorithm. Another problem is that the Larix pixels tend to be located mostly on crown edges of Larix individuals which the smaller polygons (watershed region growing algorithm) often do not fully contain. Therefore a lot more Larix pixels were counted within the watershed algorithm derived polygons compared to the smaller watershed region growing algorithm derived polygons. This may not be the best way to deal with these issues but the results seem sufficient enough for this task.

Combining field data point layer to remote sensing polygon layer

We created a column within the tree crown segmentation polygon layer where every polygon had an assigned species. In order to evaluate these classification, the remote sense derived data was combined with the field investigation data. To combine all information within the polygon layer, the field investigation data (present as a point feature layer) was joined to the polygons. The polygons were used to join all points which lay inside them. The most central laying point was chosen to assign to the polygon, other inlaying points were

subordinated. All containing data of the field investigation point feature layer was assigned to the polygon layer we need for further evaluation. This process was performed for both segmentation algorithm derived polygon layers.

Statistical evaluation

The created table was used to perform a statistical validation of the remote sensing derived data with the field data. A Pearson correlation was applied to check if the calculated tree heights are correlating with the field data tree heights. A linear regression model was applied to validate the correlation (r^2). Also the accuracies of the spectral classification and structural segmentation were calculated.

3.Results

3.1 Watershed segmentation

In the spectral classification results we can see that only in the upper plot (Fig. 15, yellow circle) section two trees were misclassified, all other trees were classified correctly (Fig. 16). From the 40 individual trees that were identified during the field investigation, only 27 individual trees were detected with the watershed segmentation algorithm. That equals a individual tree recognition rate of 67.5%. This can be traced back to the polygon sizes where in clustered tree locations more than one tree was assigned to one polygon. The spectral classification of these 27 identified trees has reached an accuracy of 92,6%. But due to the loss of 13 individuals during structural segmentation this result has to be interpreted carefully. The tree heights differ between 1.2 and 10.9 meters within the field investigation data and between 0.8 and 10.3 meters within the remote sensing derived data. The mean tree height of the field investigation data is 5.3 meters and the mean of the remote sensing derived data is 5.4 meters. The average absolute deviation is 0.4 which indicates that the tree heights between field data and remote sensing data has a accuracy variation of about 40 centimeters. Remote sensing derived tree heights are correlating ((Pearson correlation coefficient: r = 0.97) with the field investigation tree heights (Fig. 17). To validate this strong correlation a linear regression model was applied (r^2=0.95) which supports the result.

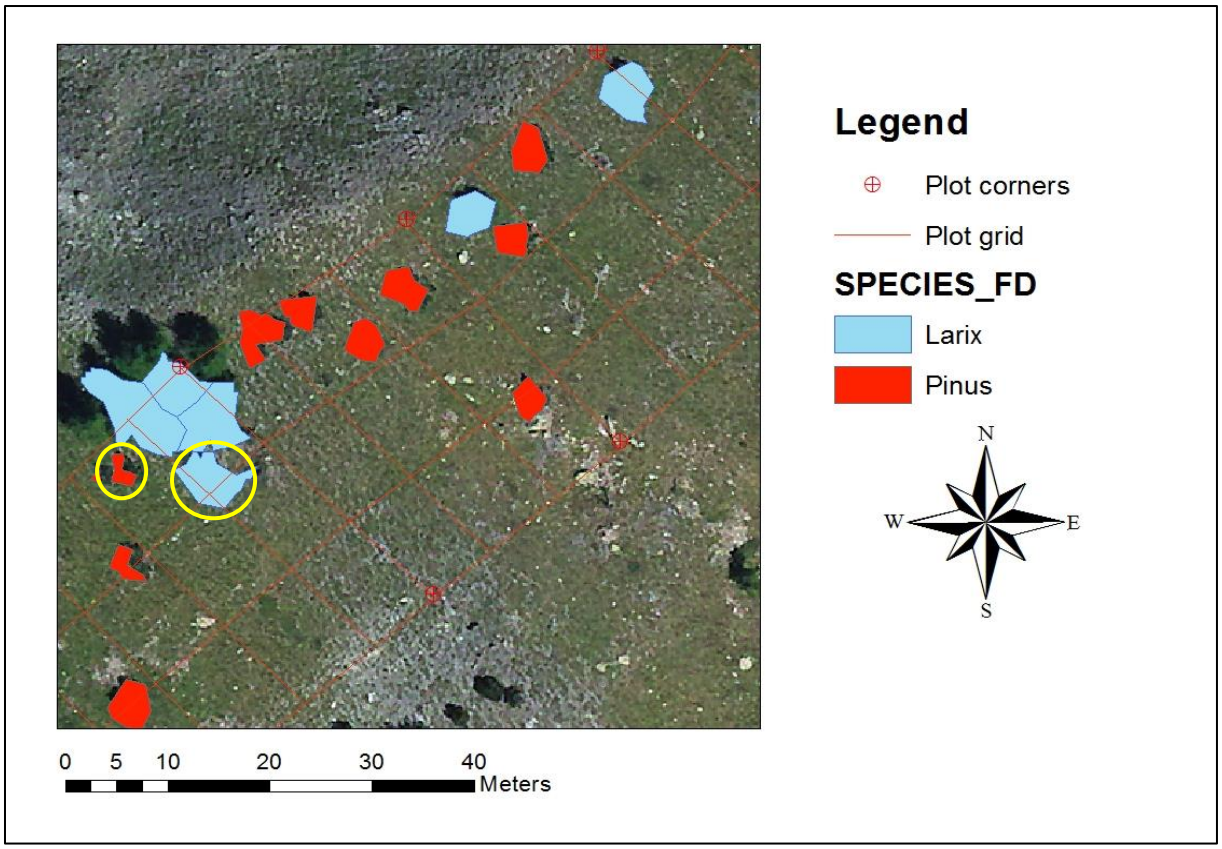

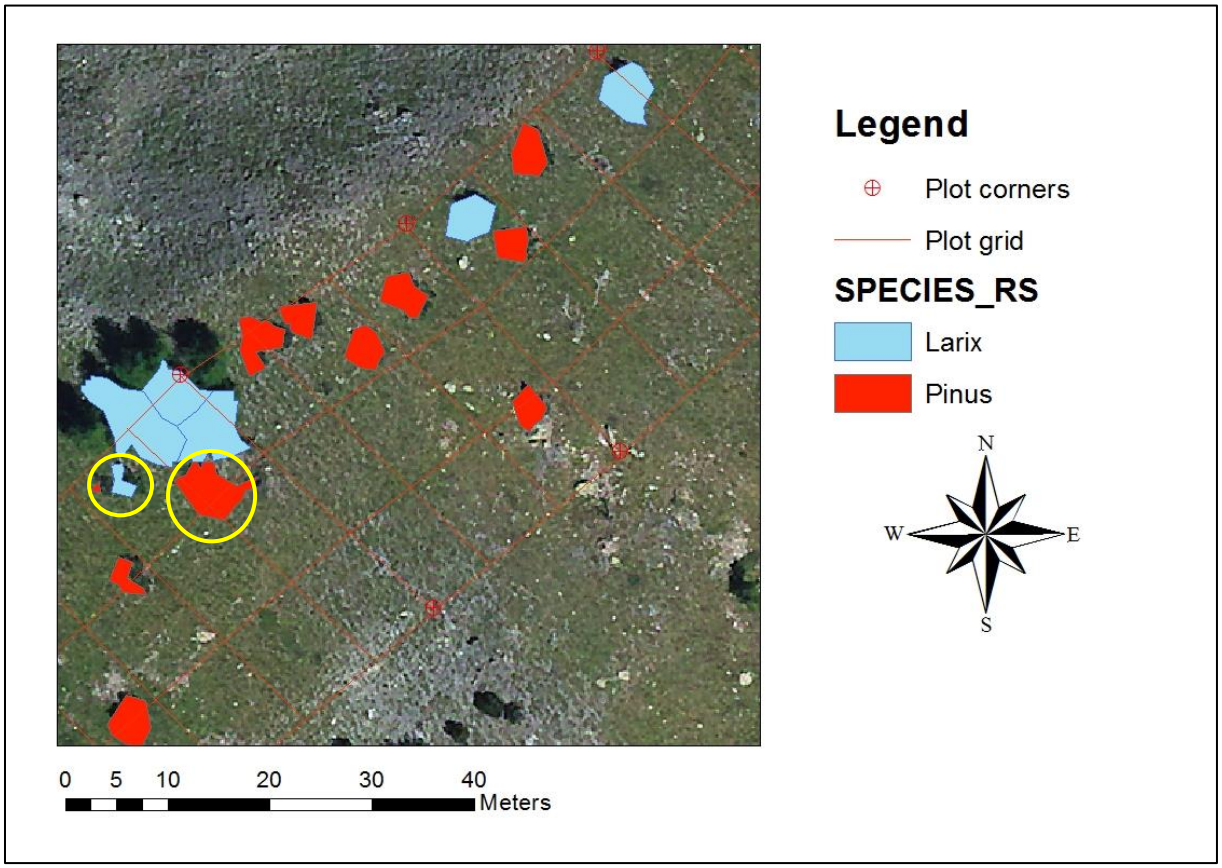

Fig. 15: Compare spectral classification in the upper plot

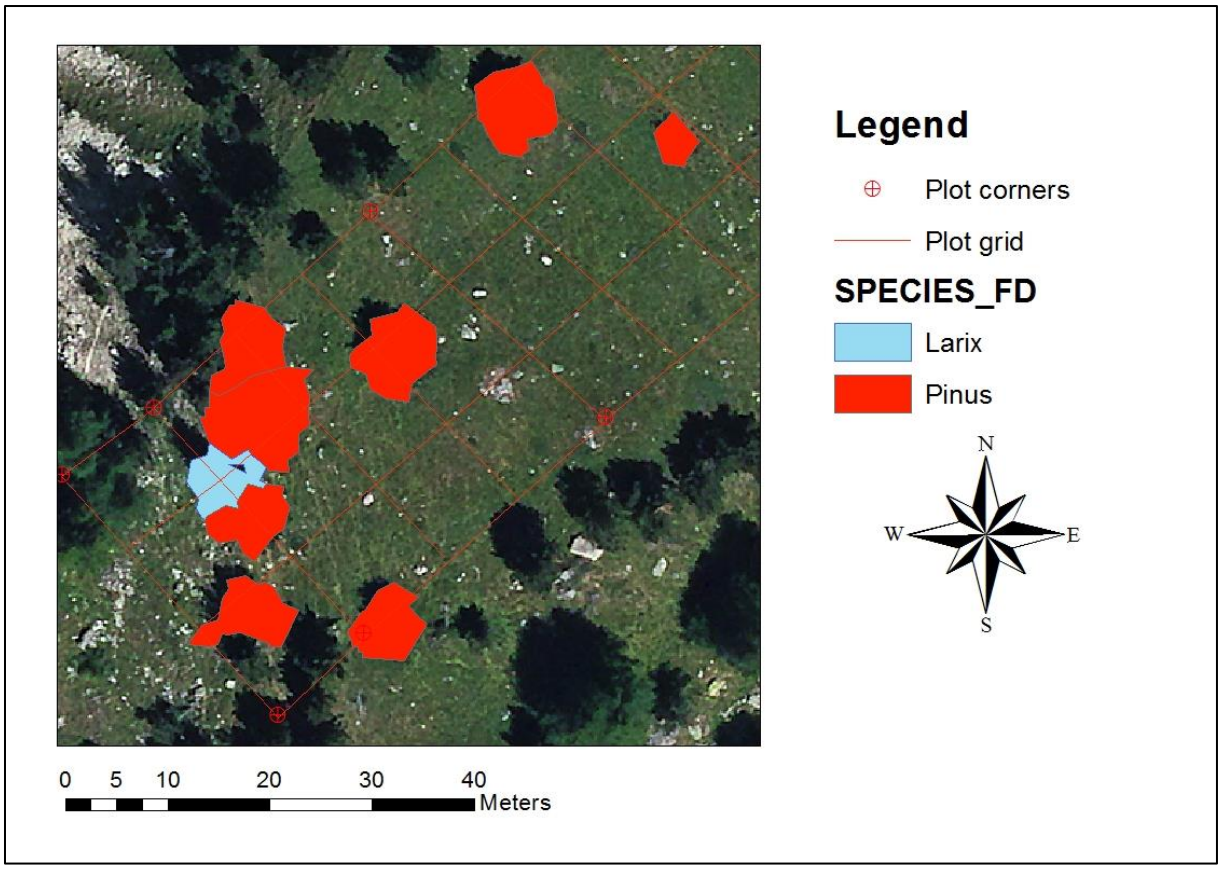

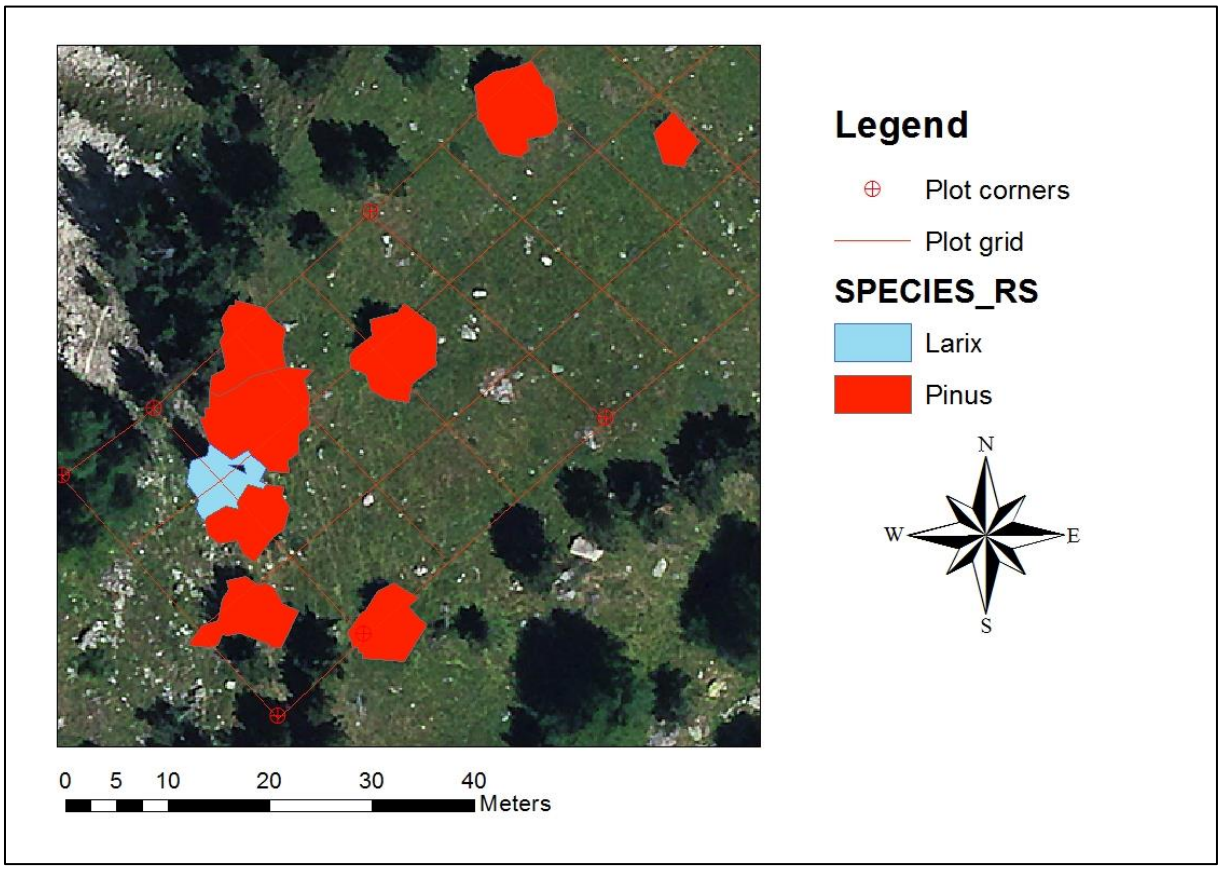

Fig. 16: Compare spectral classification in the lower plot

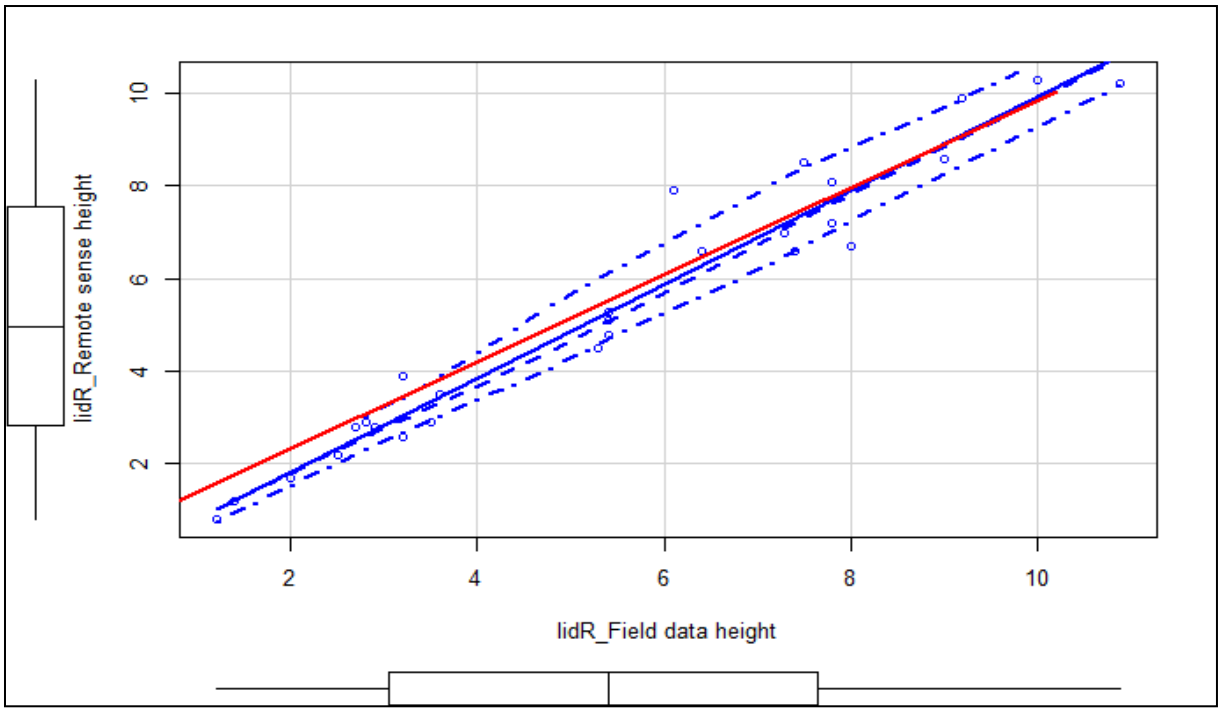

Fig. 17: Correlation of remote sensing derived data and field data

3.2 Watershed region growing segmentation

The results of the spectral classification show that two individuals in the upper plot were falsely classified (Fig. 18) and one individual in the lower plot (Fig. 19). All other trees were classified correctly. From the 40 per field investigation identified trees, 36 were detected by the watershed region growing segmentation algorithm. That equals a individual tree recognition rate of 90%, which indicated medium significance. The four missing trees occurred due to the assignment of more than one tree to a polygon and in one case due to not assigning the tree to a polygon because it laid outside of its borders. The spectral classification reached an accuracy of 91.7%. The tree heights of the field data differs between 1.2 and 11.4 meters and within the remote sensing derived data between 0.8 an 10.1 meters. The mean tree height of the field investigation data is 5.7 and the mean of the remote sensing derived data is 5.4. The average absolute deviation is 0.6 which indicates that the tree height of field and remote sense data has an accuracy variation of about 60 centimeters. Remote sensing derived tree heights are correlating (Pearson correlation coefficient: r = 0.93) with the field investigation tree heights (Fig. 20). To validate this strong correlation a linear regression model was applied (r^2=0.87) which supports the result.

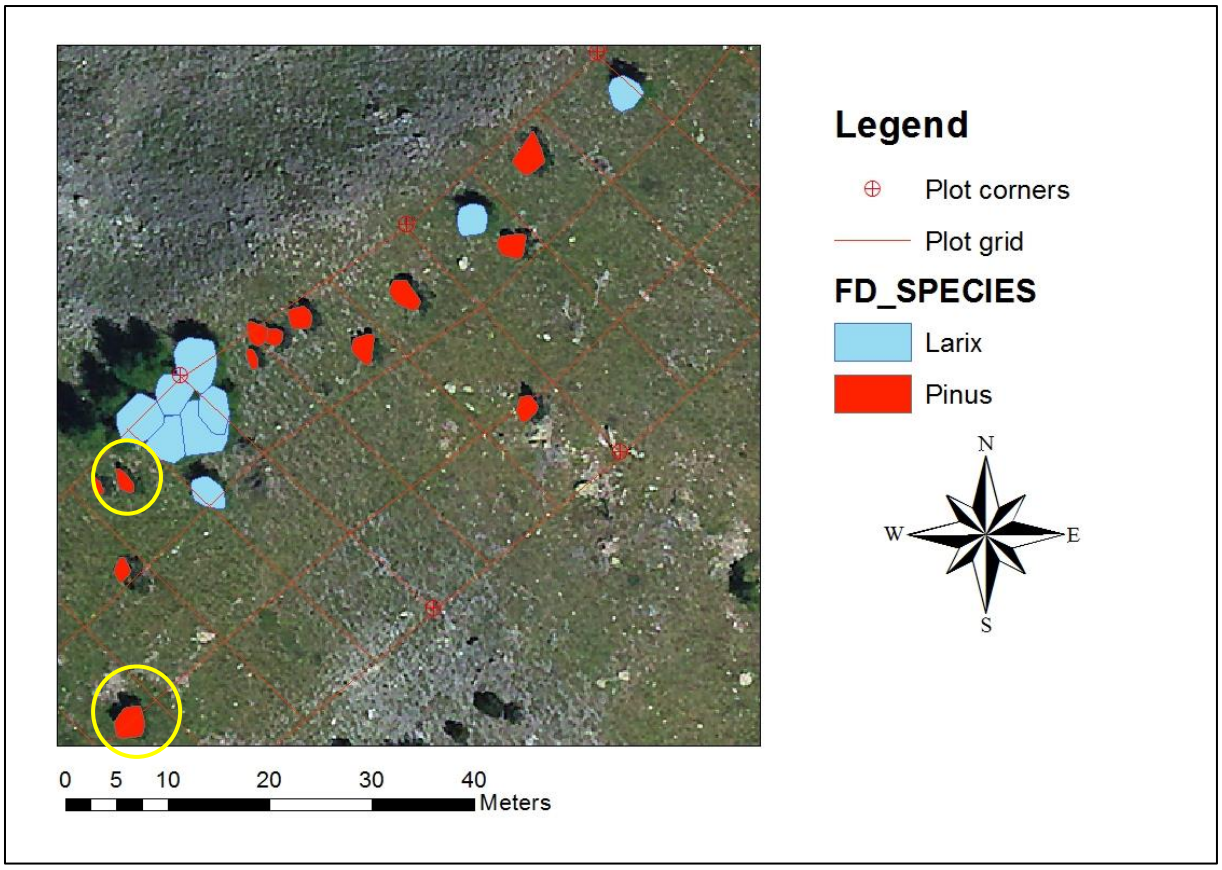

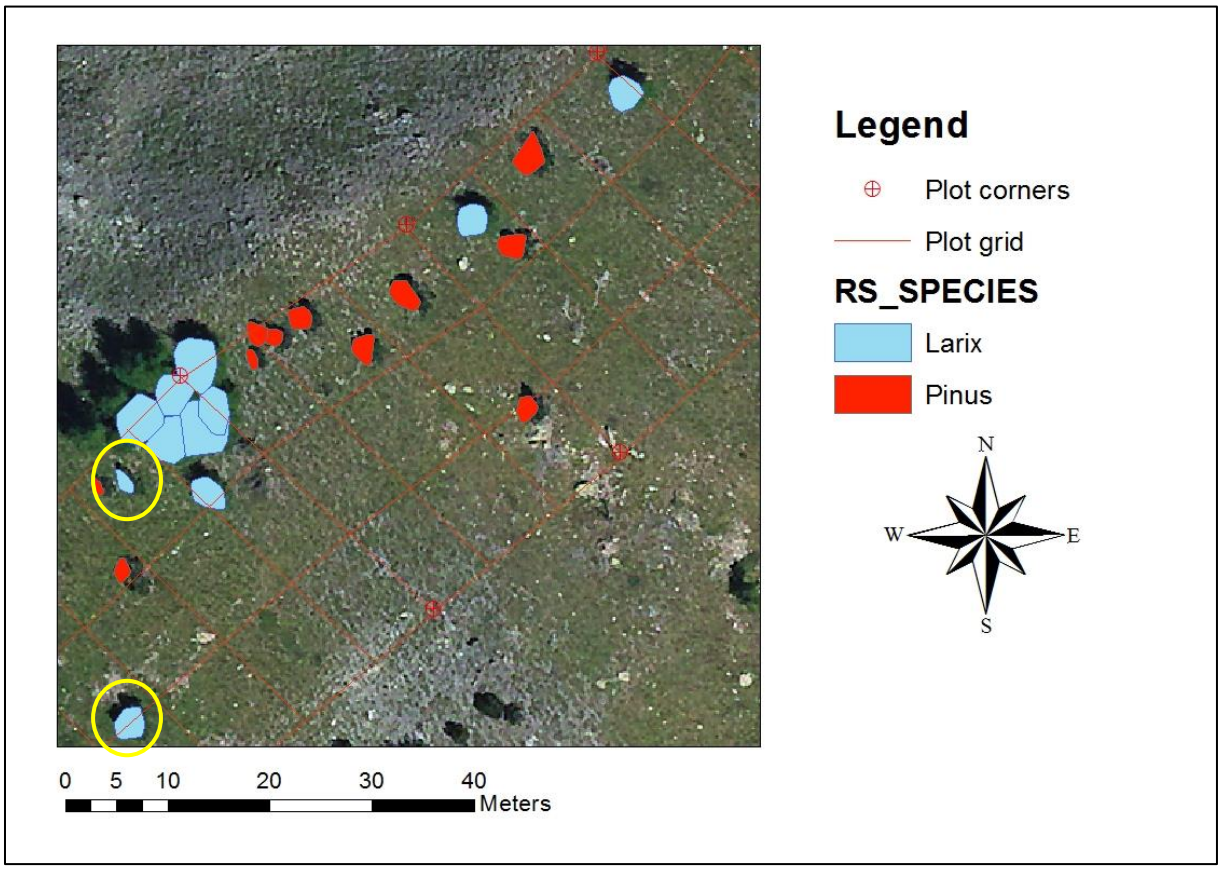

Fig. 18: Spectral classification upper plot

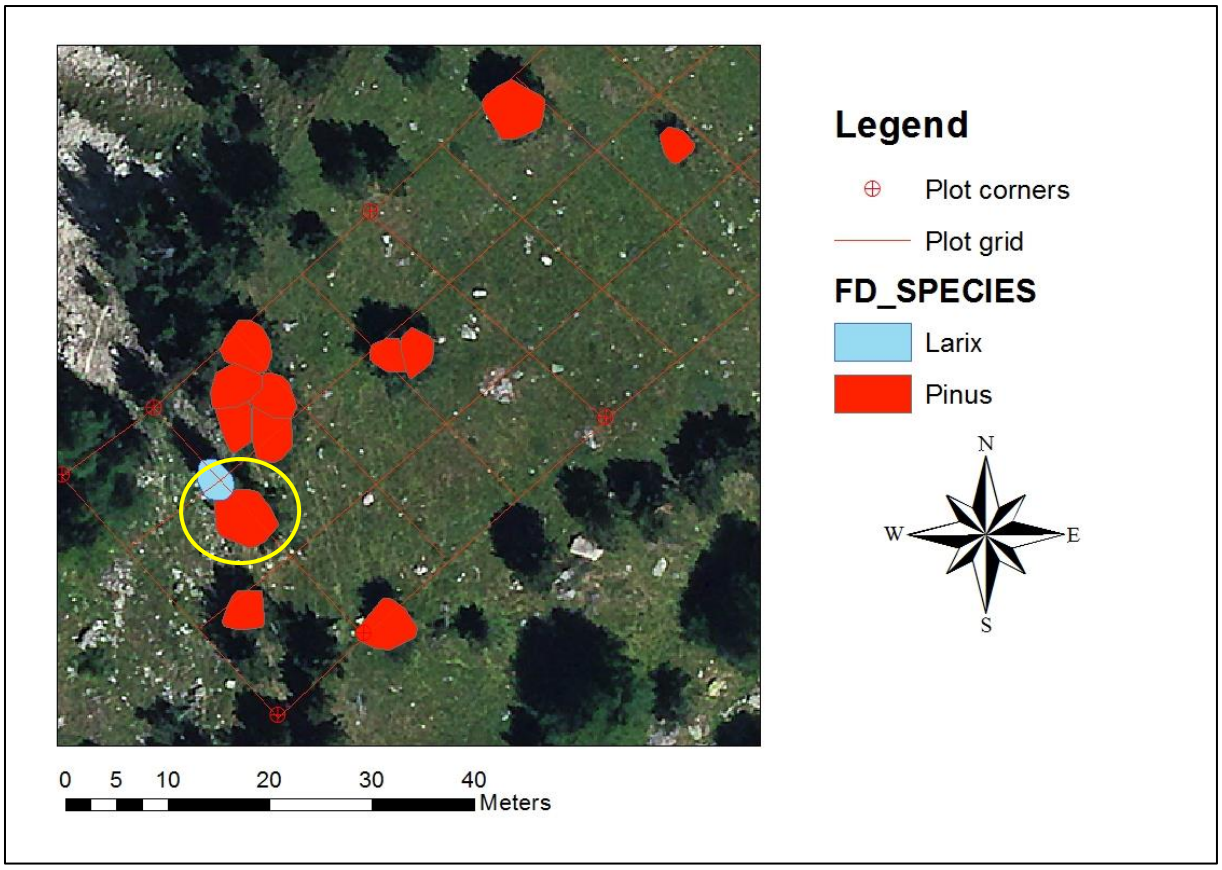

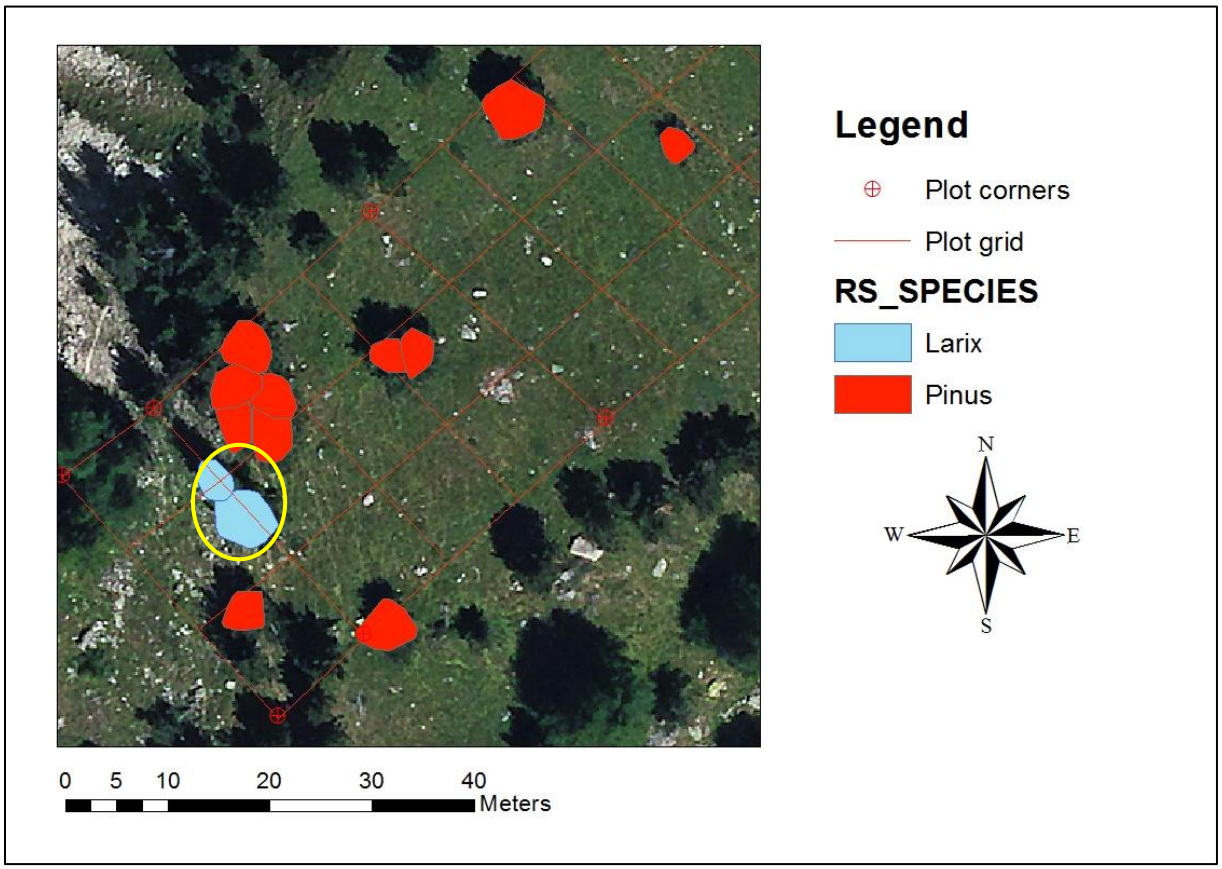

Fig. 19: Spectral classification lower plot

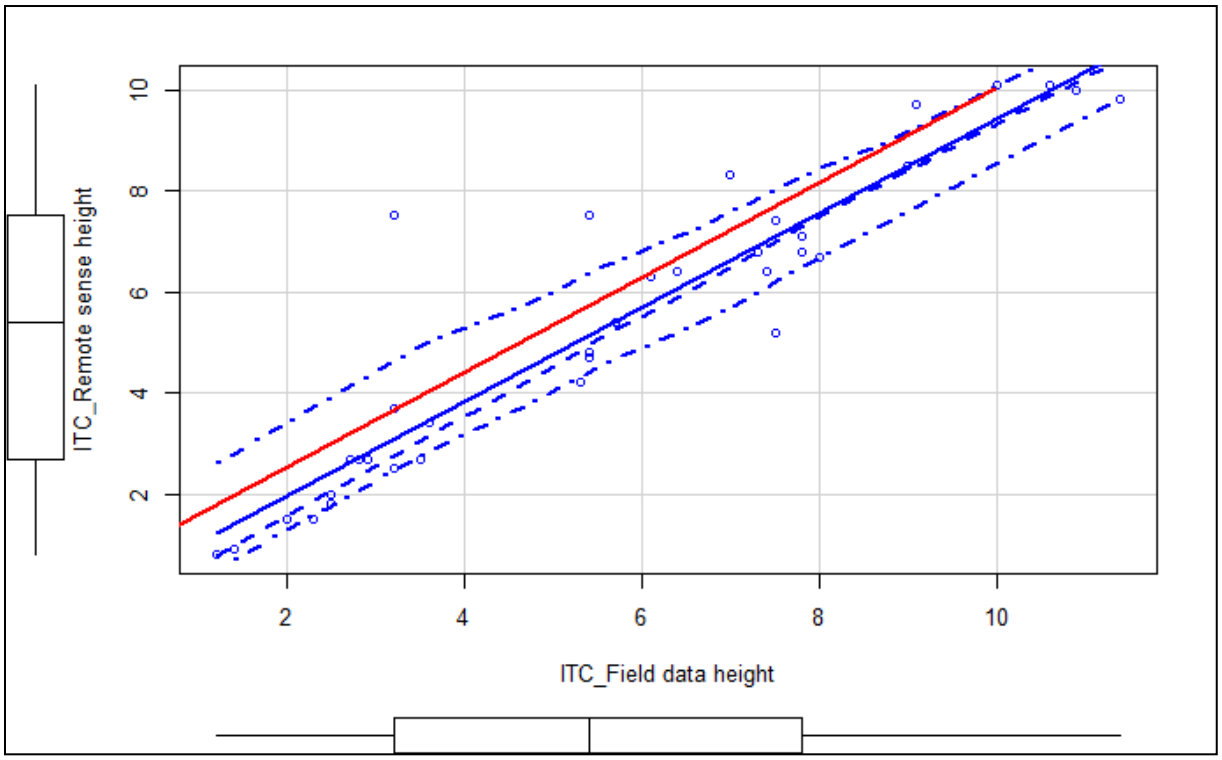

Fig. 20: Correlation of remote sensing derived data and field data

4. Discussion

Individual tree segmentation

The relatively strong spectral classification results of the watershed algorithm derived polygons can be traced back to the comparably bad results of individual tree segmentation. In this case only 27 individuals out of 40 were recognized and this leads to the comparably better spectral classification. In general the polygons were drawn much bigger than with the watershed region growing algorithm (Fig. 21).

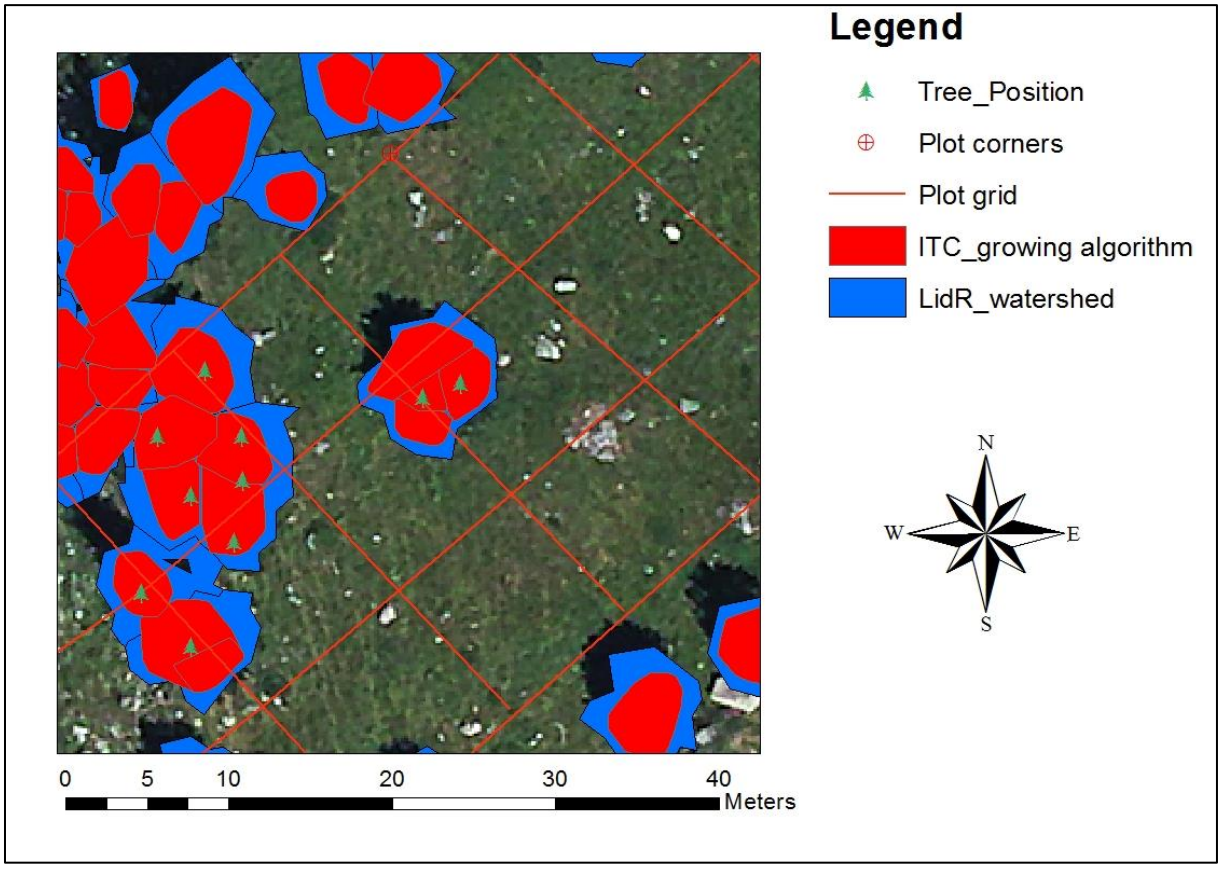

Fig. 21: Polygon size comparison

Another problem was a lack of delimiting small tree individuals. The watershed region growing algorithm was able to differentiate them better. In this case the watershed algorithm classified three small individual trees as one polygon, while the watershed region growing algorithm detected all three as separate polygons (Fig. 22, yellow circle).

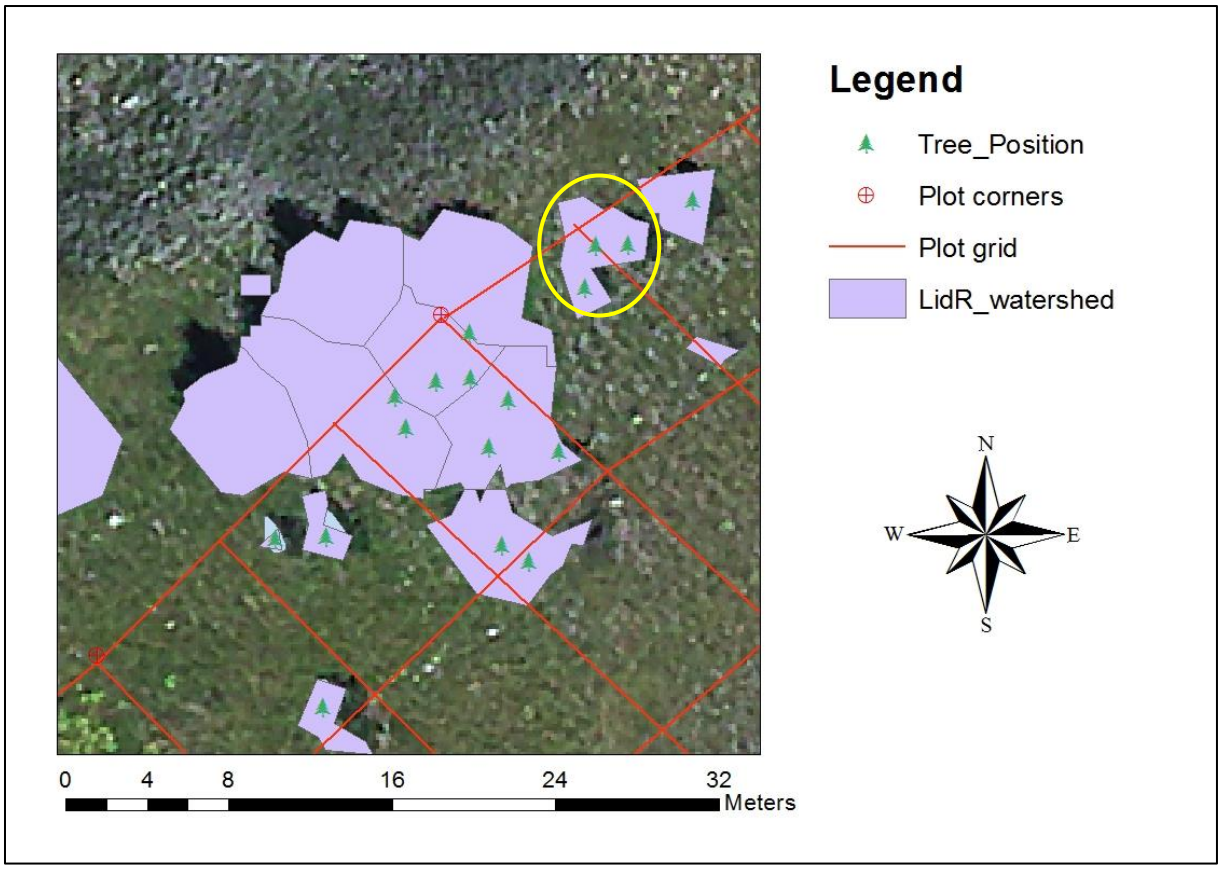

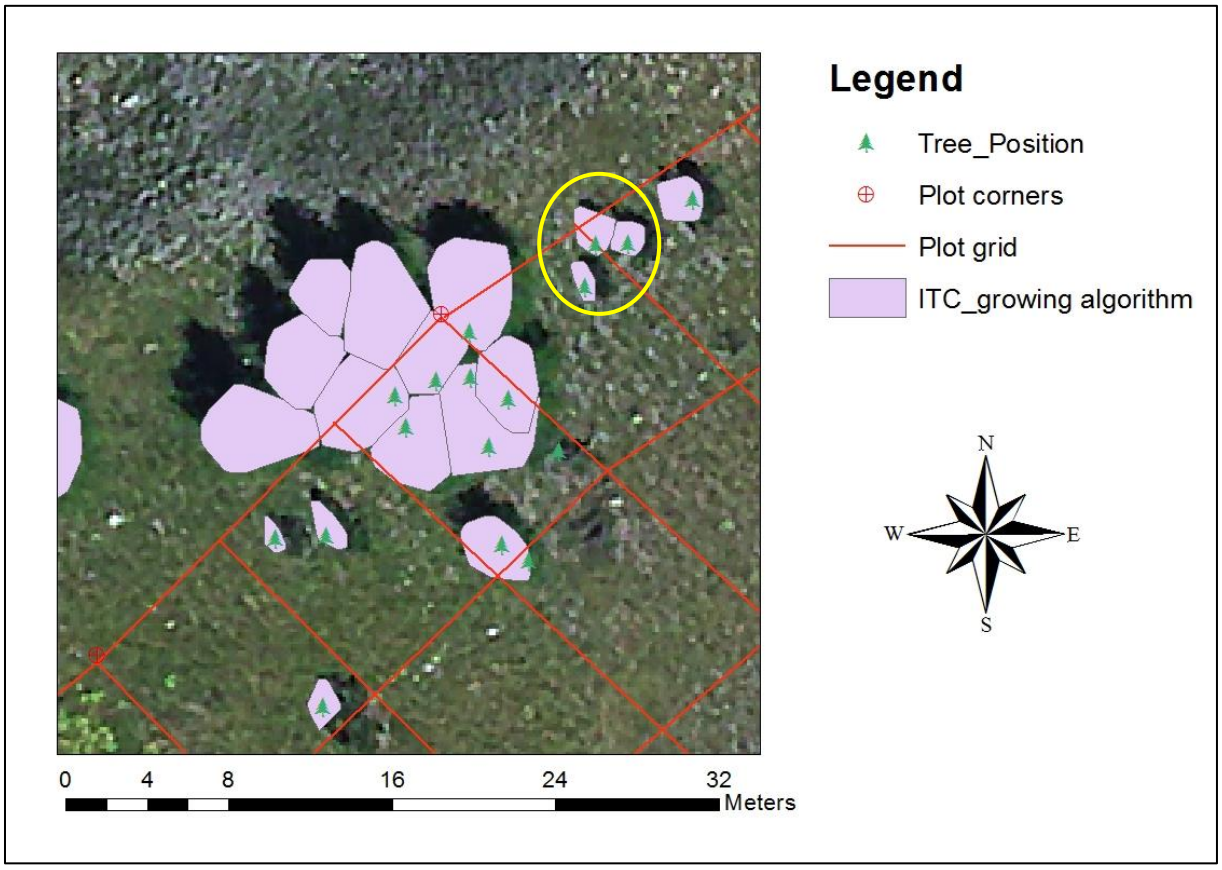

Fig. 22: Segmentation of small trees.

But the recognition of these small individuals came with the cost of false segmentation of bigger tree individuals. This leads to crown splitting of bigger trees into two or even more crowns. In this case three polygons were created because of crown splitting (Fig. 23, yellow circle). This issue is a result of the heterogeneous tree sizes within the plot. To detect local maxima, a moving window of a certain size is used. In this case we choose a size which fits well for small as well as big trees. But these algorithms were meant to segment trees in a more homogeneous environment with similar tree sizes. Therefore it is not surprising that bigger trees sometimes were split into more polygons when we were trying to detect very small trees as well.

The trees are also likely to get damaged by avalanches due to the steep slope of the plot. This could damage trees and leads to a different tree morphology with often more than one main stem per tree. This could lead to the segmentation of more than one tree because of the different crown structure.

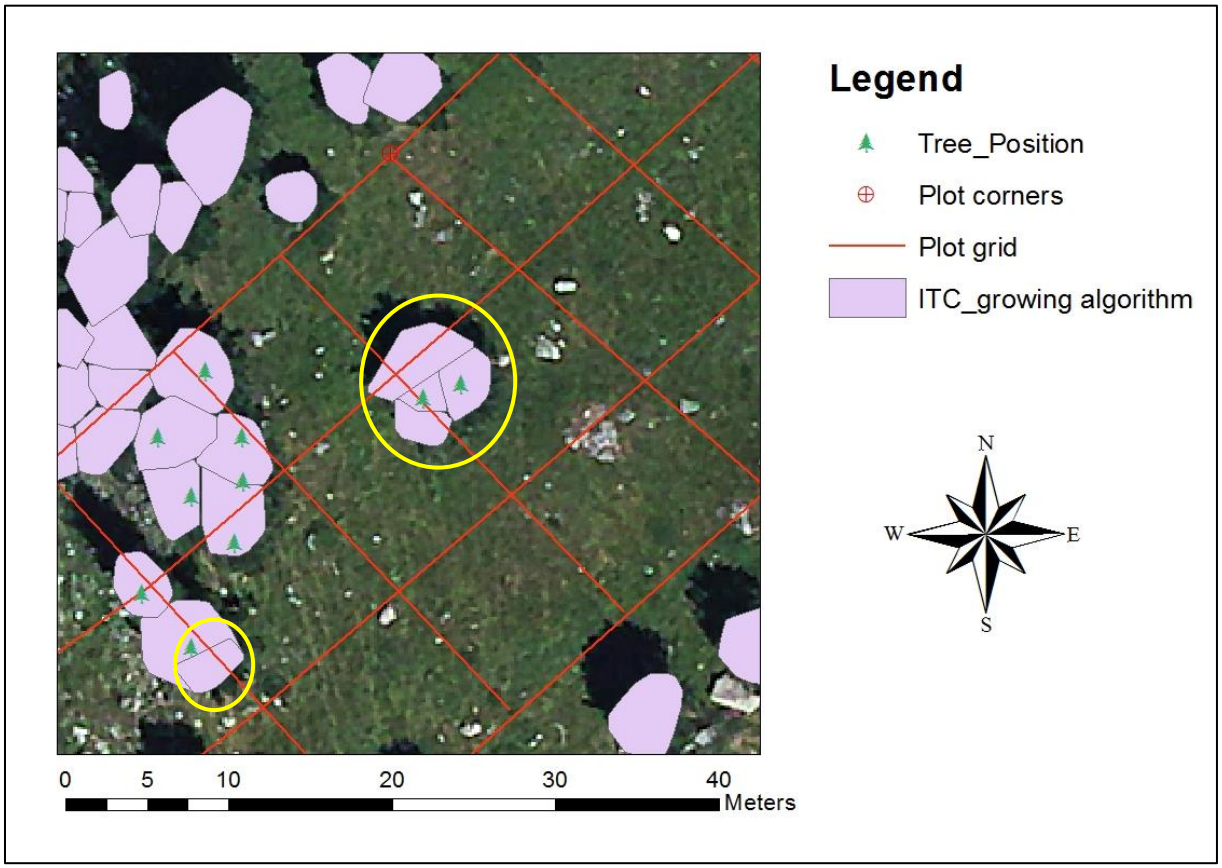

Fig. 23: Unwanted crown splitting

Structural properties

The results of the tree height comparison between field investigation and remote sensing derived data showed a strong correlation in both cases with a high significance (r^2 = 0.87/0.95). The average absolute deviation (0.6 and 0.4 meters) is mostly a result of false value assignment to the remote sensing derived polygons and recording inaccuracies during field investigation. Sometimes more than one tree was assigned to an segmented polygon which caused that sometimes false values were assigned to them. During field investigation, the tree heights were collected by using a trigonometric approach which is vulnerable to miscalculations. In general one can state that the LiDAR derived tree heights contain a similar accuracy compared to the measured tree heights during field investigation.

Spectral classification

The spectral classification of the tree species showed accuracies above 90%, which is a significant result. Even though the used classification method was not state of the art. With a more sophisticated approach it is likely to reach even better results. For example this could be done with a principle component analysis (PCA) where many artificial generated indices were used to find unique spectral properties for the occurring species. Even though the method used in this approach showed significant results it is hardly possible to use this method do delimit many different species like in temperate forests. But for the classification of alpine treelines in this area the results are promising.

All results should be interpreted carefully because of the small sample size of 40 trees and the relatively small plot size. This is not an amount which suits to predict the complexity of nature. The results should be seen as an indicator for the possibilities of remote sensing. To allow more meaningful interpretations, more plots need to be examined in similar locations to increase the sample size to an significant amount which allows more general predictions.

5. Conclusion

To conclude the results one can state that the watershed region growing segmentation algorithm performed much better for this approach than the basic watershed segmentation algorithm. Especially small trees were detected very accurately compared to the watershed method. In general, the detection rate of individual trees was 22.5% higher than the basic watershed method. Although the spectral classification results were higher than the ITC segmentation method, this result had no significance due to the high misclassification rate of the segmentation process. The only reason for a higher classification rate is the lower number of polygons corresponding to the combination of many trees in one polygon.

The comparison between the tree heights showed a significant correlation for both segmentation algorithms. The heterogeneity of the plot is a challenge. Not only the occurrence of very small and big trees is hard to handle with a stable moving window approach to detect local maxima, also the crown structure is in some cases hard to interpret due to tree crippling caused by avalanches and other factors in this environment. Also the structure of the vegetation is very heterogeneously distributed. There a big separately standing trees with usual undamaged crowns. They were mostly segmented correctly with both segmentation methods. There are big separately standing trees with more than one main stem and unusual looking crowns. These were often segmented falsely with more than one polygon with the watershed region growing algorithm and reliable with the basic watershed method. There are very small separately standing trees which were segmented reliably by the watershed region growing algorithm and significantly worse with the basic watershed method. And there are medium sized trees and big trees growing in clusters. These vegetation form was better segmented by the watershed region growing algorithm but is still far from a significant result. This is mainly caused by the special morphology of the trees. The plot position is very steep and especially young trees get damaged a lot which is the reason for their unusual morphology.

In spite of the plots heterogeneity, the results of the watershed region growing algorithm were quietly accurate. Maybe a good way to solve some of the issues we encountered is to split the segmentation, so the moving window can be customized to detect small and big trees separately. But this needs to be supervised. Finally we can conclude that the structural and spectral classification of tree individuals can be performed with a high accuracy but

depends on the homogeneity of the vegetation. Although some parameters like the tree age and others have to be gathered by field investigation, remote sensing data can save expenditures and provides a comparable data quality for some parameters. It could be used to predict the tree species with a high accuracy. Also the tree heights can be determined accurately. This makes it a valuable tool to monitor alpine treelines. It could be used to detect new established seedlings or recently died trees without the need to go to the location physically. But this would presuppose an continuous data access and regular renewal of existing remote sensing data. All reached results must be handled with care concerning the development of universal statements about alpine treelines. The plot and sample size is too low to allow general statements. But the results can be seen as an indicator for the possibilities of remote sensing derived predictions. To allow general assumptions the sample size needs to be increased.

Literature

- **COOMES, D. A. ET AL. (2017):** Area-based vs. tree-centric approaches to mapping forest carbon in Southeast Asian forests from airborne laser scanning data. In: Remote Sensing of Environment 194 77-88: doi: https://doi.org/10.1016/j.rse.2017.03.017
- **DALPONTE M., REYES F., KANDARE K., GIANELLE D. (2015):** Delineation of Individual Tree Crowns from ALS and Hyperspectral data: a comparison among four methods. In: European Journal of Remote Sensing, Vol. 48, pp. 365-382. doi: https://doi.org/10.5721/EuJRS20154821
- **DALPONTE M., BRUZZONE L., VESCOVO L., GIANELLE D. (2009):** The role of spectral resolution and classifier complexity in the analysis of hyperspectral images of forest areas. In: Remote Sensing of Environment, 113: 2345-2355. doi: https://doi.org/10.1016/j.rse.2009.06.013
- **DEB K., ASHRAFUL S. (2014):** Shadow Detection and Removal Based on YCbCr Color Space. In: The Smart Computing Review. 4. 10.6029/smartcr.2014.01.003.Internet sources:https://www.researchgate.net/publication/263662695_Shadow_Detection_and_Removal_Based_on_YCbCr_Color_Space (Access: 11.11.18)
- **ENE L., NÆSSET E., GOBAKKEN T. (2012):** Single tree detection in heterogeneous boreal forests using airborne laser scanning and area-based stem number estimates. International Journal of Remote Sensing, 33 (16): 5171-5193. doi: https://doi.org/10.1080/01431161.2012.657363
- **GRAFSTRÖM A., RINGVALL A.H. (2013):** Improving forest field inventories by using remote sensing data in novel sampling designs. Canadian Journal of Forest Research, 43: 1015- 1022. doi: https://dx.doi.org/10.1139/cjfr-2013-0123
- **HARSCH M., HULME P., MCGLONE M., DUNCAN R. (2009):** Are treelines advancing? A global meta-analysis of treeline response to climate warming. Ecology Letters. Ecology letters. 12. doi: https://doi.org/10.1111/j.1461-0248.2009.01355.x
- **HYYPPÄ J., KELLE O., LEHIKOINEN M., INKINEN M. (2001):** A segmentation-based method to retrieve stem volume estimates from 3-D tree height models produced by laser scanners. IEEE Transaction on Geoscience and Remote Sensing, 39: 969-975. doi: https://dx.doi.org/10.1109/36.921414
- **ISENBURG M. (2018**): LAStools: Rapidlasso: https://rapidlasso.com/lastools/ (Access: 22.11.18)
- **KAARTINEN, H. ET AL. (2012):** An international comparison of individual tree detection and extraction using airborne laser scanning. In: Remote Sensing, 4(4), pp. 950–974. doi: https://doi.org/10.3390/rs4040950
- **KHOSRAVIPOUR, A. ET AL. (2013):** Development of an algorithm to generate a Lidar pit - free canopy height model. In: Proceedings of Silvilaser2013 : 13th International

conference on Lidar applications for assessing forest ecosystems, October, 9-11, 2013 Beijing, China, p. Paper SL2013-030, pp. 125–128.

- **KOCH, B., HEYDER, U. AND WEINACKER, H. (2006):** Detection of Individual Tree Crowns in
  Airborne Lidar Data. In: Photogrammetric Engineering & Remote Sensing,72(4), pp. 357ff. doi: https://doi.org/10.14358/PERS.72.4.357
- **MOHAN, M. ET AL. (2017):** Individual tree detection from unmanned aerial vehicle (UAV) derived canopy height model in an open canopy mixed conifer forest. In: Forests, 8(9). doi: https://doi.org/10.3390/f8090340
- **NATUR 4.0 (2018):** Sensing Biodiversity. Philipps University Marburg. Department of Geography: Source: https://www.uni-marburg.de/de/fb19/natur40 (Access: 19.11.18)
- **OTSU N. (1979)** : A Threshold Selection Method from Gray-Level Histograms. IEEE Transaction on Systems, Man and Cybernetics, 9 (1): 62-66. doi: https://dx.doi.org/10.1109/TSMC.1979.4310076
- **PAN Y., BIRDSEY R., PHILLIPS O.L., JACKSON R.B. (2013):** The Structure, Distribution, and Biomass of the World's Forests. In: Annual Review of Ecology, Evolution, and Systematics, 44: pp. 593-622.
  doi: https://dx.doi.org/10.1146/annurev-ecolsys-110512-135914
- **POPESCU, S. C. AND WYNNE, R. H. (2004):** Seeing the Trees in the Forest : Using Lidar and Multispectral Data Fusion with Local Filtering and Variable Window Size for Estimating Tree Height. In: Photogrammetric Engineering & Remote Sensing, 70(5), pp. 589–604. doi: https://doi.org/10.14358/PERS.70.5.589
- **REUDENBACH, C. (2018a):** Crown Segmentation on Canopy Height Models from low budget UAV generated digital terrain models. Source: https://github.com/gisma/uavRst/wiki/Crown-Segementation-on-Canopy-Height-Models-from-low-budget-UAV-generated-digital-terrain-models models (Access: 22.11.18)
- **REUDENBACH, C. (2018b):** ITC Segmentation: Source: https://github.com/gisma/uavRst/blob/master/man/chmseg_ITC.Rd (Access: 22.11.18)
- **ROUSSEL J. (2018a):** lidR-Package:
  Source: https://github.com/Jean-Romain/lidR (Access: 22.11.18)
- **ROUSSEL J. (2018b):** lidR-Package: Catalog-index:
  Source: https://github.com/Jean-Romain/lidR/blob/master/R/catalog_index.r (Access: 22.11.18)
- **ROUSSEL J. (2018c):** lidR-Package: lastrees:
  Source: https://github.com/Jean-Romain/lidR/blob/master/R/lastrees.r (Access: 22.11.18)

- **SOLOMON, S., QIN, D., MANNING, M., CHEN, Z., MARQUIS, M., AVERYT, K.B., TIGNOR, M. & MILLER, H.L. (EDS.) (2007):** Climate change 2007. In: The physical science basis. Cambridge University Press, Cambridge.
- **TRENT UNIVERSITY LIBRARY MAPS, DATA & GOVERNMENT INFORMATION CENTRE (MADGIC) (2014):** Watershed Delineation with ArcGIS 10.2.x Source:https://www.trentu.ca/library/sites/default/files/documents/WatershedDelineation_10_2.pdf (Access: 21.11.18)
- **ZHANG, K., CHEN, S. C., WHITMAN, D., SHYU, M. L., YAN, J., & ZHANG, C. (2003):** A progressive morphological filter for removing nonground measurements from airborne LIDAR data. In: IEEE Transactions on Geoscience and Remote Sensing, 41(4 PART I), 872–882. doi: https://doi.org/10.1109/TGRS.2003.810682

Erklärung

Hiermit versichere ich, dass ich die vorliegende Arbeit selbständig verfasst und keine anderen als die angegebenen Quellen und Hilfsmittel benutzt habe.

Die Bachelorarbeit wurde in der jetzigen oder einer ähnlichen Form noch bei keiner anderen Hochschule eingereicht und hat noch keinen sonstigen Prüfungszwecken gedient.

Datum: _____ Unterschrift: _____